(2)

FREE ELECTRON LASER WITH HIGH CURRENT DENSITY THERMIONIC CATHODE

FINAL TECHNICAL REPORT

FOR THE PERIOD

JANUARY 1, 1989 TO OCTOBER 31, 1989

CONTRACT No.: N00014-89-J-1417 REPORT No. 5

SPONSOR: OFFICE OF NAVAL RESEARCH
PHYSICS DIVISION, CODE 412
ARLINGTON, VA 22217

PROJECT DIRECTOR: PROFESSOR WARD D. GETTY

UM ACCOUNT No.: 026138 No. of Pages: 49

Graduate Student Assistants: Marc E. Herniter
Kelly D. Pearce
Ronald Temske

Undergraduate Assistant: Oleh Karpenko

THE UNIVERSITY OF MICHIGAN

Department of Electrical Engineering and Computer Science
Ann Arbor, Michigan 48109-2122
USA

SECURITY CLASSIFICATION OF THIS PAGE (When Data Entered)

REPORT DOCUMENTATION PAGE

READ INSTRUCTIONS BEFORE COMPLETING FORM

1. REPORT NUMBER: 5	2. GOVT ACCESSION NO.
3. RECIPIENT'S CATALOG NUMBER	
4. TITLE (and Subtitle): Free Electron Laser with High Current Density Thermionic Cathode, Final Technical Report for the period January 1, 1989 to October 31, 1989	5. TYPE OF REPORT & PERIOD COVERED: Final Technical Report January 1, 1989-October 31,1989
	6. PERFORMING ORG. REPORT NUMBER
7. AUTHOR(s): Ward D. Getty, Kelly D. Pearce and Ronald R. Temske	8. CONTRACT OR GRANT NUMBER(s): ONR Grant No. N00014-89-J-1417
9. PERFORMING ORGANIZATION NAME AND ADDRESS: University of Michigan, Dept. Electrical Engineering & Computer Science, Ann Arbor, Michigan 48109	10. PROGRAM ELEMENT PROJECT, TASK AREA & WORK UNIT NUMBERS: 61153N, RR 011-09-01, NR 012-760
11. CONTROLLING OFFICE NAME AND ADDRESS: Office of Naval Research, Physics Division, Code 412, Arlington, VA 22217	12. REPORT DATE: July 15, 1991
	13. NUMBER OF PAGES: 49
14. MONITORING AGENCY NAME & ADDRESS(if different from Controlling Office): Same	15. SECURITY CLASS. (of this report): Unclassified
	15a. DECLASSIFICATION/ DOWNGRADING SCHEDULE

16. DISTRIBUTION STATEMENT (of this Report)

Approved for public release; distribution unlimited

17. DISTRIBUTION STATEMENT (of the abstract entered in Block 20, if different from Report)

Same as Report

18. SUPPLEMENTARY NOTES

NONE

19. KEY WORDS (Continue on reverse side if necessary and identify by block number)

electron beams, gyrating electron beams, wigglers, electron guns, thermionic cathodes

20. ABSTRACT (Continue on reverse side if necessary and identify by block number)

An electron gun with a lanthanum hexaboride planar cathode is used to generate a gyrating electron beam by passing the beam through a wiggler electromagnet in an axial guide field. The beam test stand, Marx generator, wiggler design, and beam diagnostics are described in detail.

DD FORM 1 JAN 73 1473 EDITION OF 1 NOV 65 IS OBSOLETE

S/N 0102-LF-014-6601

UNCLASSIFIED

SECURITY CLASSIFICATION OF THIS PAGE (When Data Entered)

TABLE OF CONTENTS

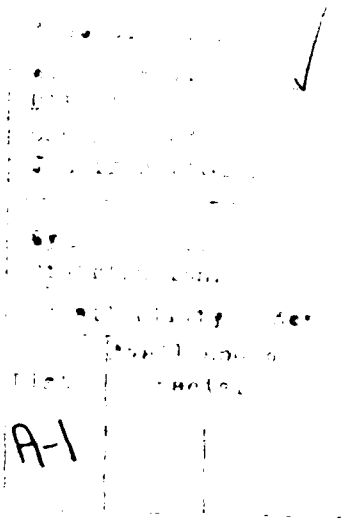

FINAL TECHNICAL REPORT

ONR CONTRACT No. N00014-89-J-1417

FREE ELECTRON LASER WITH HIGH CURRENT DENSITY THERMIONIC CATHODE

1. INTRODUCTION

1.1 General Background

The period covered by this report was mainly a rebuilding period between the completion of one Ph.D. thesis project and the start of another. The completed thesis was that of Marc E. Herniter and was entitled "A Bombardment Heated LaB_6 Thermionic Cathode Electron Gun." This work was mainly on the development of a Pierce-type electron gun with a lanthanum hexaboride (LaB_6) cathode. The next project was to use this electron gun to produce a gyrating electron beam in an axial guide magnetic field. The application of this beam would be in the area of free-electron lasers or cyclotron harmonic masers.

Major modifications in the experimental apparatus were necessary to develop the capability of generating and diagnosing this electron beam.

1.2 List of Papers, Theses, Graduate Students, and Reports

Journal Article

(1) "Pulsed Cathode Heating Method," G. A. Lipscomb, M. E. Herniter, and W. D. Getty, *IEEE Trans. on Plasma Science*, Vol. PS-17, pp. 898-905 (December 1989).

Conference Papers

(1) "Transport of a 120-*kV*, 100-*A* Electron Beam From a LaB_6 Cathode Through combined Wiggler and Axial Magnetic Fields," K. D. Pearce and W. D. Getty, Thirty-First Annual Meeting, Division of Plasma Physics, *Amer. Phys. Soc.*, Anaheim, California, November 13-17, 1989.

Theses

(1) M. E. Herniter, "A Bombardment Heated LaB_6 Thermionic Cathode Electron Gun," Ph.D. Thesis, Department of Electrical Engineering and Computer Science, The University of Michigan, Ann Arbor, Michigan, 1989.

(2) G. A. Lipscomb, "Pulsed Cathode Heating Method," M.S.E. Thesis, Department of Electrical Engineering and Computer Science, The University of Michigan, Ann Arbor, Michigan, 1989.

Graduate Students

Marc E. Herniter, Ph.D. (Electrical Engineering), 1989

George A. Lispcomb, M.S.E. (Electrical Engineering), 1989

Ronald R. Temske, M.S.E. (Nuclear Engineering)

Kelly Pearce, Ph.D. (Nuclear Engineering)

Undergraduate Student

Oleh Karpenko, Nuclear Engineering

Report

"High-Current-Density Thermionic Cathodes and the Generation of High-Voltage Electron Beams," Final Technical Report for the period, September 1, 1982 to April 30, 1989; ONR Contract No. N00014-82-K-0448, Ward D. Getty, Marc E. Herniter, George A. Lipscomb, and Kelly D. Pearce, Department of Electrical Engineering and Computer Science, The University of Michigan, Ann Arbor, MI 48109-2122.

1.3 General Plan of Final Report

Section 2 of this report will describe the work done on system modifications and development of new diagnostics. Section 3 describes thewiggler design, construction, and testing. Section 4 summarizes the work accomplished in this period. The appendix contains absuracts of papers and a copy of a report written on the wiggler work.

2. SYSTEM MODIFICATIONS

2.1 Marx Generator

The Marx generator contained four 0.08 μF capacitors connected as a 4-stage Marx bank. In order to make the voltage droop in the 5-μs voltage pulse smaller, the capacitors were changed to four 0.22 μF capacitors. Originally, four were used but this placed a lower limit of 100 *kV* on the output voltage since 25 *kV* was needed to fire the spark gaps. Later, one stage was removed to allow operation down to 75 *kV*. Figure 1 shows an inverted voltage pulse when the crowbar spark gap was not used to terminate the pulse at 5 μs.

In earlier work, it was found to be impossible to prevent the trigger generator on the crowbar spark gap from firing prematurely due to noise pickup so the crowbar was not used in the work of M.E. Herniter.[1] The crowbar spark gap was changed to a 3-electrod Maxwell Model 40359 irradiation triggered spark gap, and a Maxwell Model 40230 100-*kV* trigger generator was used to trigger it. After the proper trigger circuit was developed, it was found that this crowbar system worked quite well. An example of a crowbarred voltage pulse is shown in Fig. 2. Initially, some difficulty was experienced with triggering the new spark gap because both a 250-*pF* coupling capacitor and a trigger-initiation gap (TIG) were used in series in the firing pin circuit and the trigger voltage was dividing across them. When the capacitor was removed, the system worked properly. The complete Marx generator circuit is shown in Fig. 3.

2.2 Vacuum System

The vacuum system was modified because it was necessary to mount axial guide field coils. The direction of flow of the electron beam was changed from vertical to horizontal, and the drift tube and analyzer sections were added. A small turbopump was placed on the analyzer end to provide pumping at both ends of the low-conductance drift tube. These changes required a major amount of time because the analyzer section had to be able to hold the 100-*kV* retarding potential.

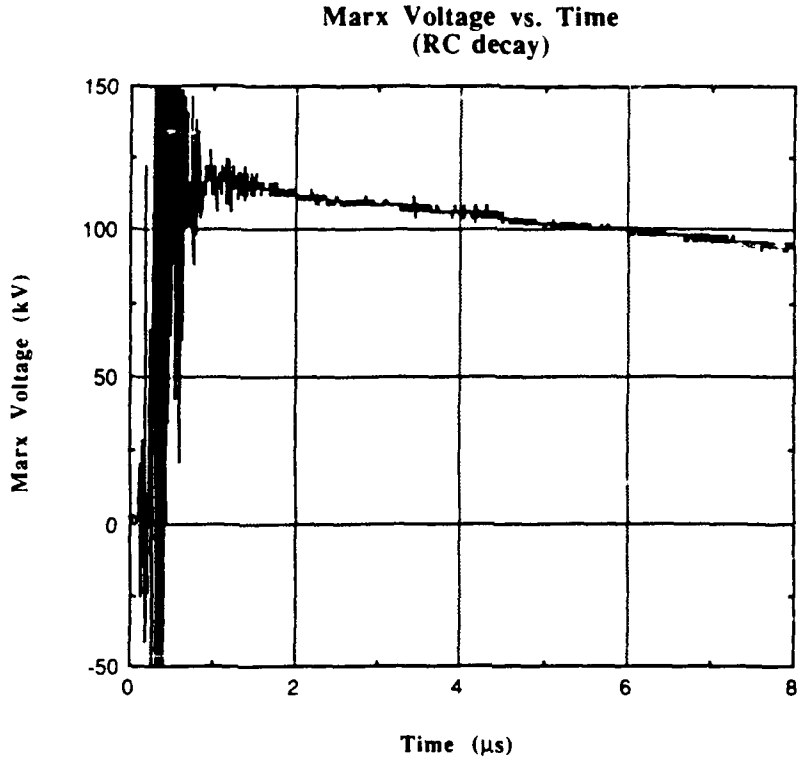

Figure 1: Marx voltage pulse (inverted) when crowbar is not used.

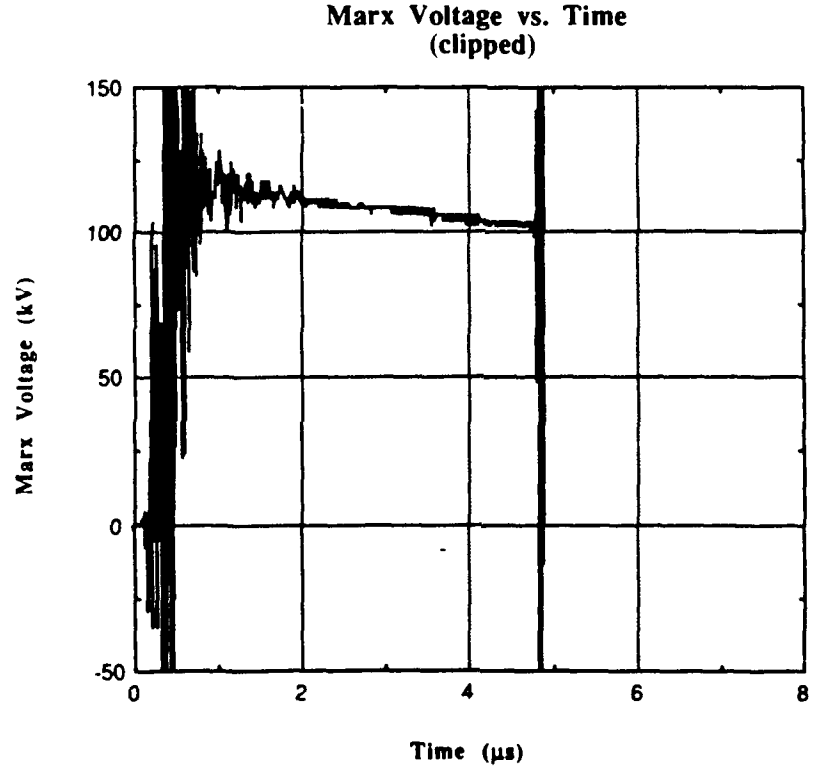

Figure 2: Marx voltage pulse (inverted) when crowbar fired successfully.

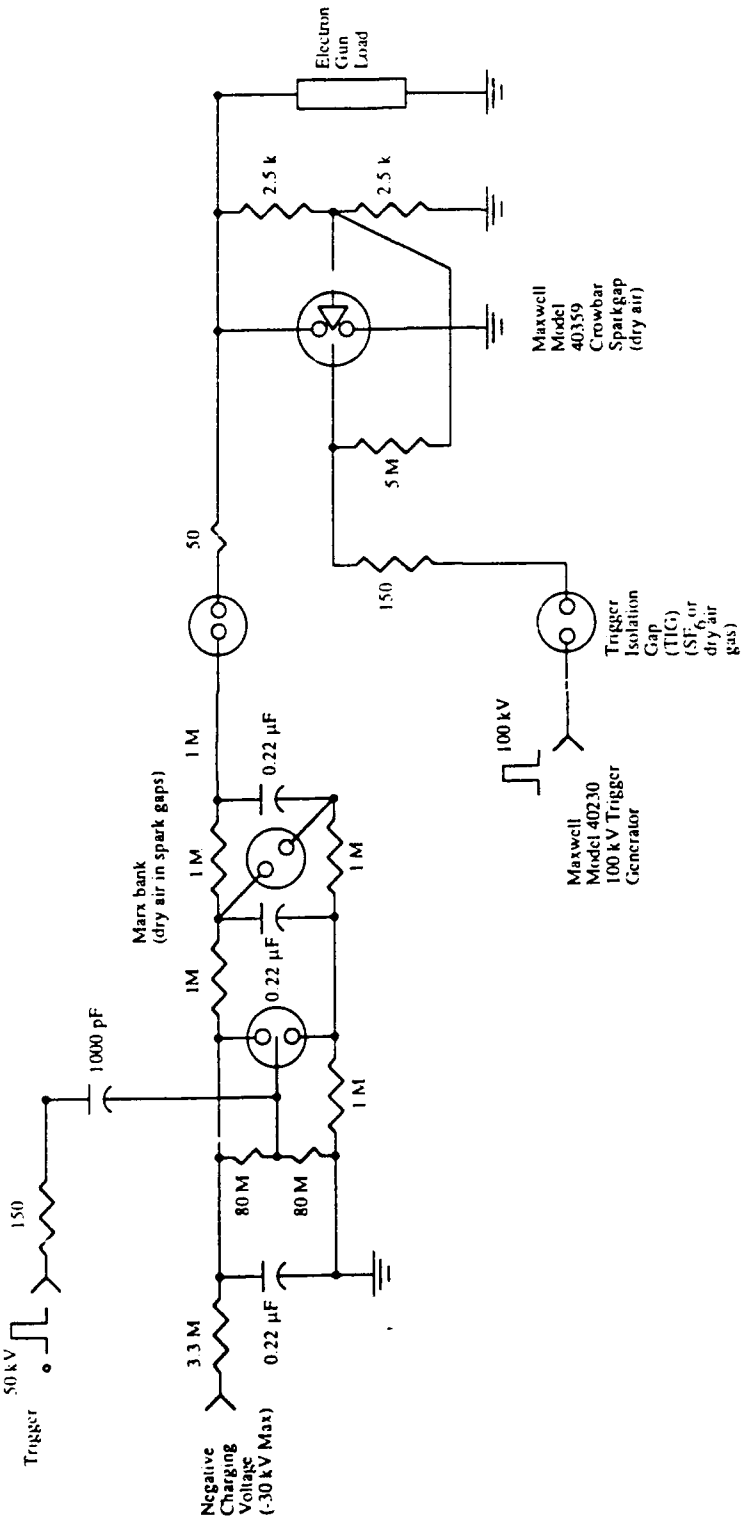

Figure 3: Three-stage Marx generator with maximum output voltage of 90 *kV*. The modified TIG circuit for the crowbar switch is also shown.

Failures were also experienced with the power supply of the new turbopump and one of the new mechanical backing pumps. The rebuilt system is shown in Fig. 4. A control panel was built to control all 4 vacuum pumps and protect them against power outages or cooling-water loss.

2.3 Magnetic Field

Aluminum stands were built to hold the magnetic field coils. In order to obtain the desired axial magnetic field shape, six large circular coils and a small solenoid were used. Four of the six large coils are water cooled so a water system had to be installed. Three power supplies were obtained to power these seven electromagnets.

A crucial test was performed as soon as the coils were in place to determine if the bombardment heating system for the LaB_6 cathode would operate in the 1100-G axial guide field. The electron gun is totally immersed in the field. Two concerns were that the magnetic field would cause the tungsten filament to deform, causing uneven bombardment power deposition or a short circuit between the cathode and filament. A second concern is that even if the filament didn't deform, the magnetic field would focus the bombarding electrons and cause uneven heating.

Fortunately, none of these problems occurred and the bombardment heating system operated satisfactorily. The final computed and measured magnetic field profiles $B_z(z)$ are shown in Figs. 5 and 6. The coil system is capable of going up to an axial field of 1200 G without overheating. Some differences are found between the measured and calculated fields because of steel endplates in the solenoid which are not accounted for in the calculation. The shape of the field near the cathode was adjusted to match the best conditions found with the SLAC EGUN code.[2] Results of the SLAC simulation are shown in Fig. 7.

2.4 Retarding Potential Analyzer

A major effort was mode to develop electrodes for the retarding potential analyzer (RPA) which could be used to 120 kV, and to analyze electron trajectories through the analyzer. Figure 4 shows the general layout of the analyzer. It is of the filter lens type[3] and has only one electrode at the voltage of the electron beam accelerating voltage. This electrode is identified as the "filter lens" in Fig. 4. This electrode is connected to a corona-free lead wire and terminal that go to a negative

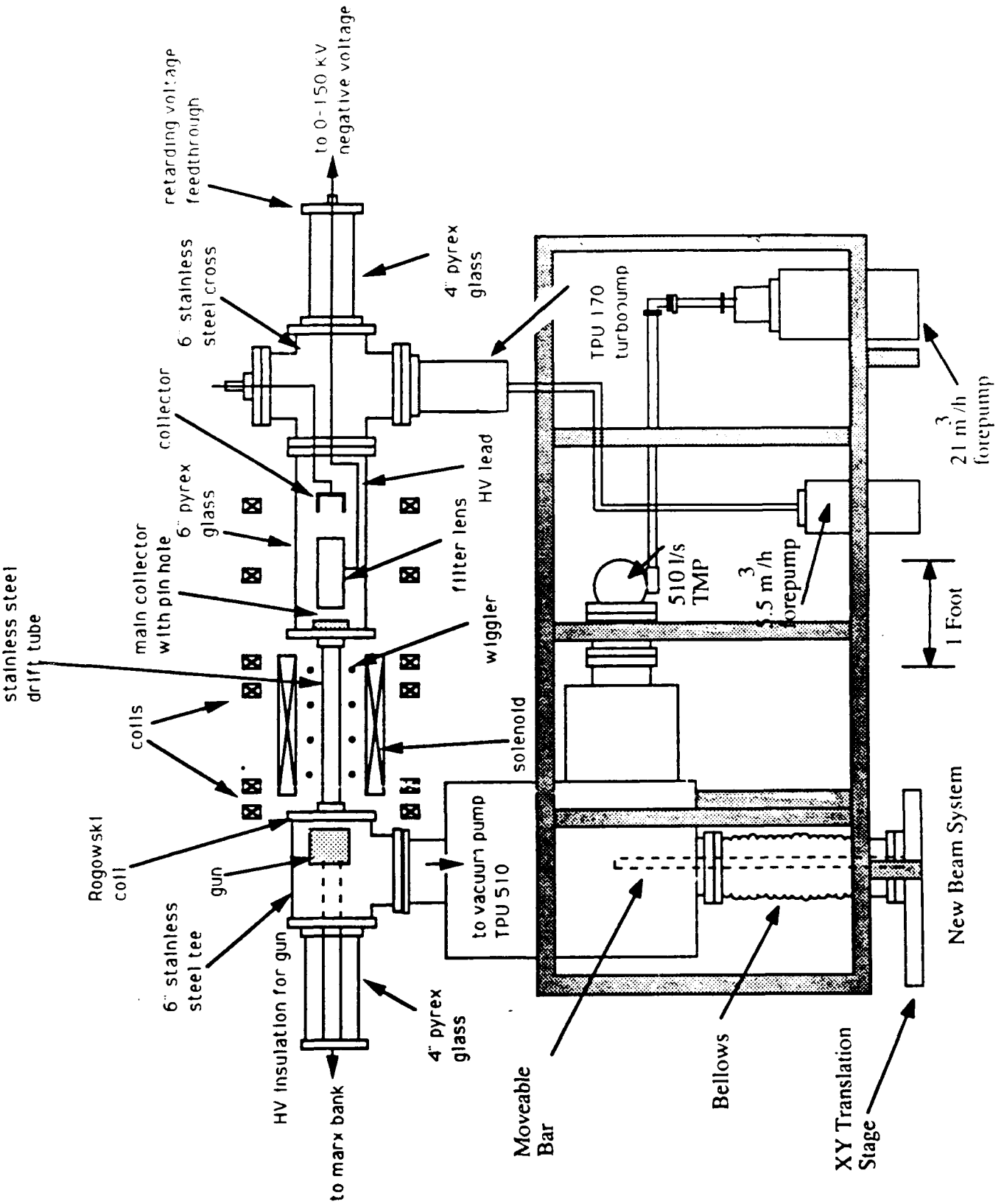

Figure 4: New vacuum system dubbed "SUREFIRE" with expanded 6-inch diameter glass tube for housing the velocity analyzer.

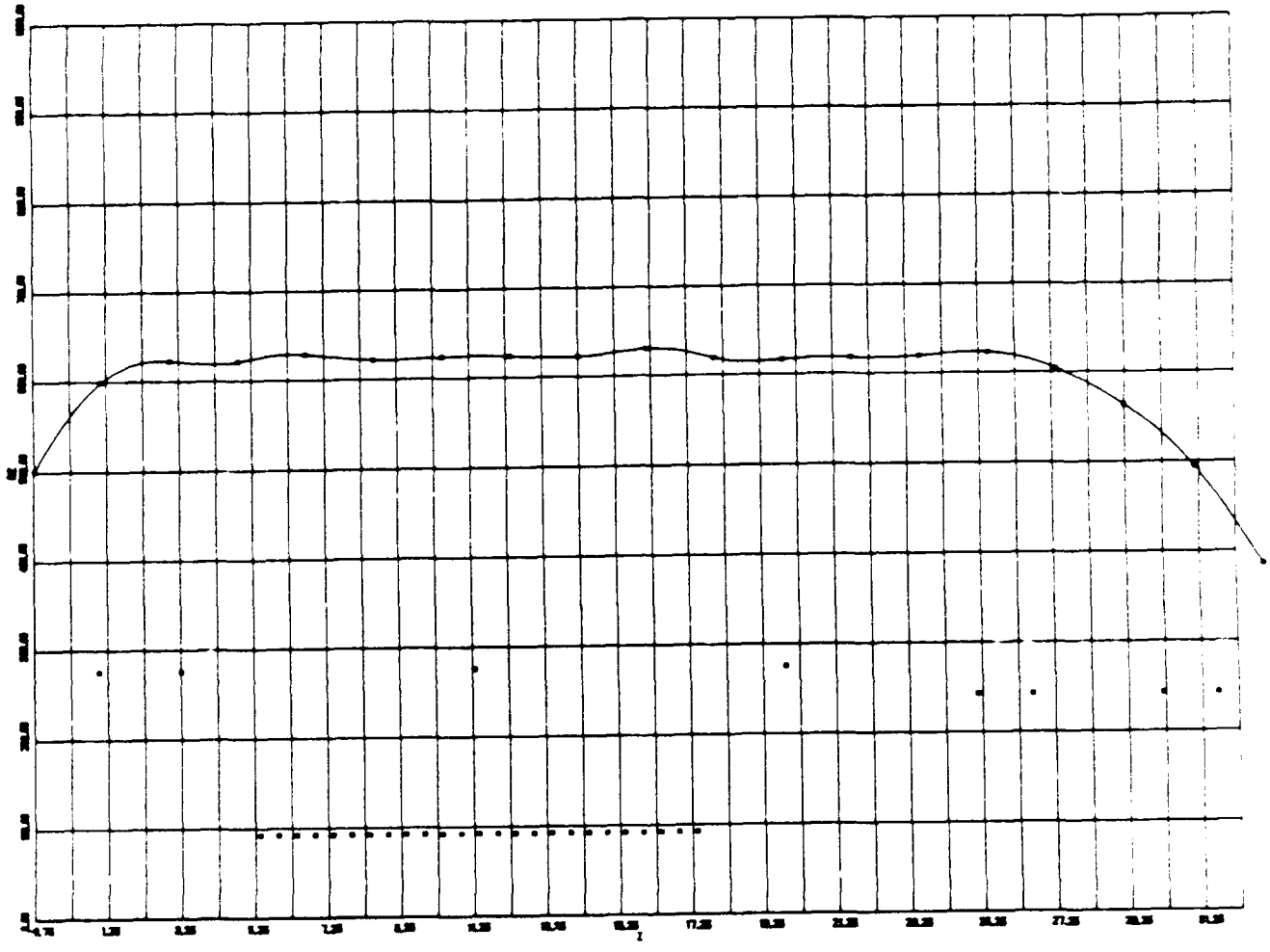

Figure 5 Computed magnetic field using filament models for the coils. This coil configuration was found by trial-and-error. The dots represent filament coils. The two pairs of filaments at $z \geq 24$ represent two coils. The 25 filaments in the center model the solenoid.

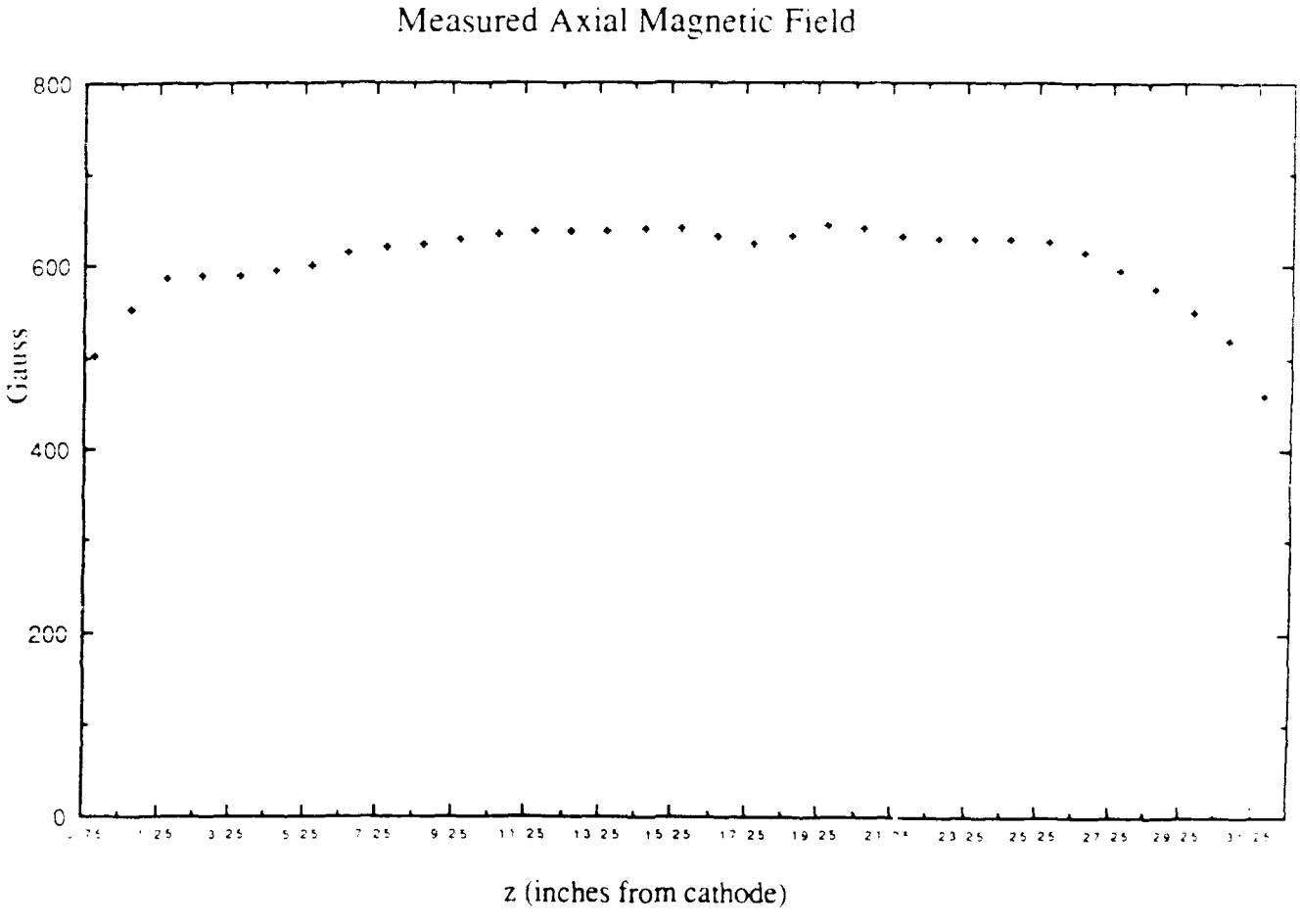

Figure 6 Measured field $B_z(z)$ for the optimum coil positions and currents. Steel in the solenoid casing causes a significant difference from the calculated field.

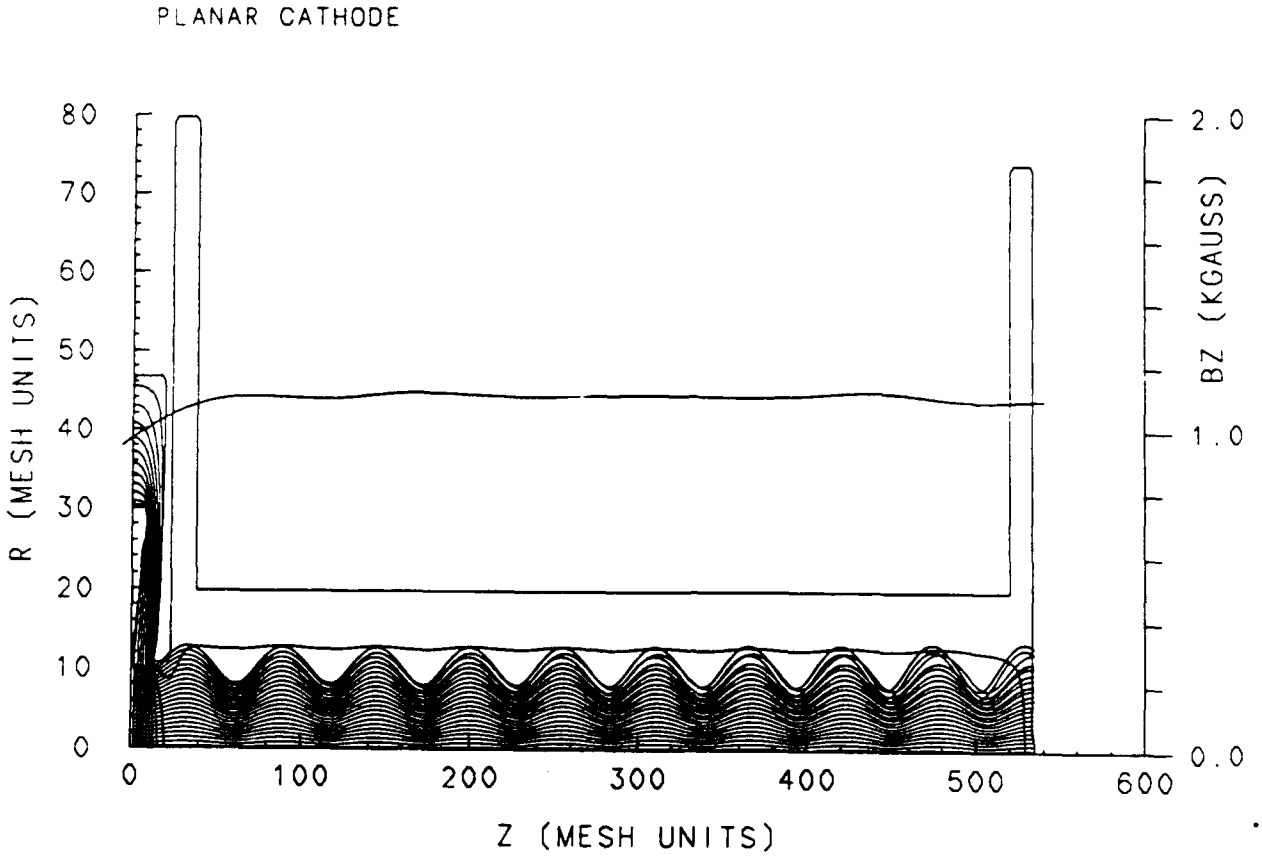

Figure 7: Example of SLAC EGUN simulation for the drift region and gun.

0-150 *kV* dc power supply. A detailed drawing of the RPA is shown in Fig. 8. The collector electrode is a coaxial structure with a grounded outside shield tube surrounding an insulated inner cup.

The operation of the RPA was analyzed with the EGUN code. Electrons with various initial velocity vectors ($v_\perp$, $v_\parallel$) are admitted to the analyzer for various negative voltages applied to the filter lens. Results showing the discriminatory operation of the analyzer for various conditions are shown in Figs. 9, 10, and 11. The RPA was found to be able to discriminate between two electrons with the same total energy but different values of $v_\perp/v_\parallel$ as shown by Figs. 9 and 10.

2.5 Miscellaneous Developments

The electron gun used by Herniter[1] was found to be too undependable for obtaining analyzer curves above 75 *kV* because of arcing. This electron gun is shown in Fig. 12 and is approximately 4 inches in diameter. The gun was enlarged to 5.375 inches in diameter and smooth triple points were machined at all vacuum-metal-insulator joints. The cathode stalk was the same in both guns. A drawing of the larger gun is shown in Fig. 13. The new gun worked up to approximately 100 *kV*, but dependable consistent operations were obtained only up to 80-85 *kV*.

A resistance voltage divider was built and calibrated for the 5-μs, 100-*kV* pulse. The calibration was done with a Velonex high-voltage pulser and a Tektronix high-voltage scope probe. The results are shown in Fig. 14. A Rogowski coil for the beam current at the gun anode aperture was built and calibrated with a Pearson transformer, but its sensitivity was too low to allow it to be used in the experiment. Gun cathode current was measured with a Pearson transformer and current through the drift tube was measured with a collector plate.

Other tasks accomplished in this period were the setup and checkout of the 150-*kV* power supply for the RPA, the installation of doors and interlocks around the experiment, and the installation of lead shielding for x-ray protection on the end of the area where personnel exposure was possible.

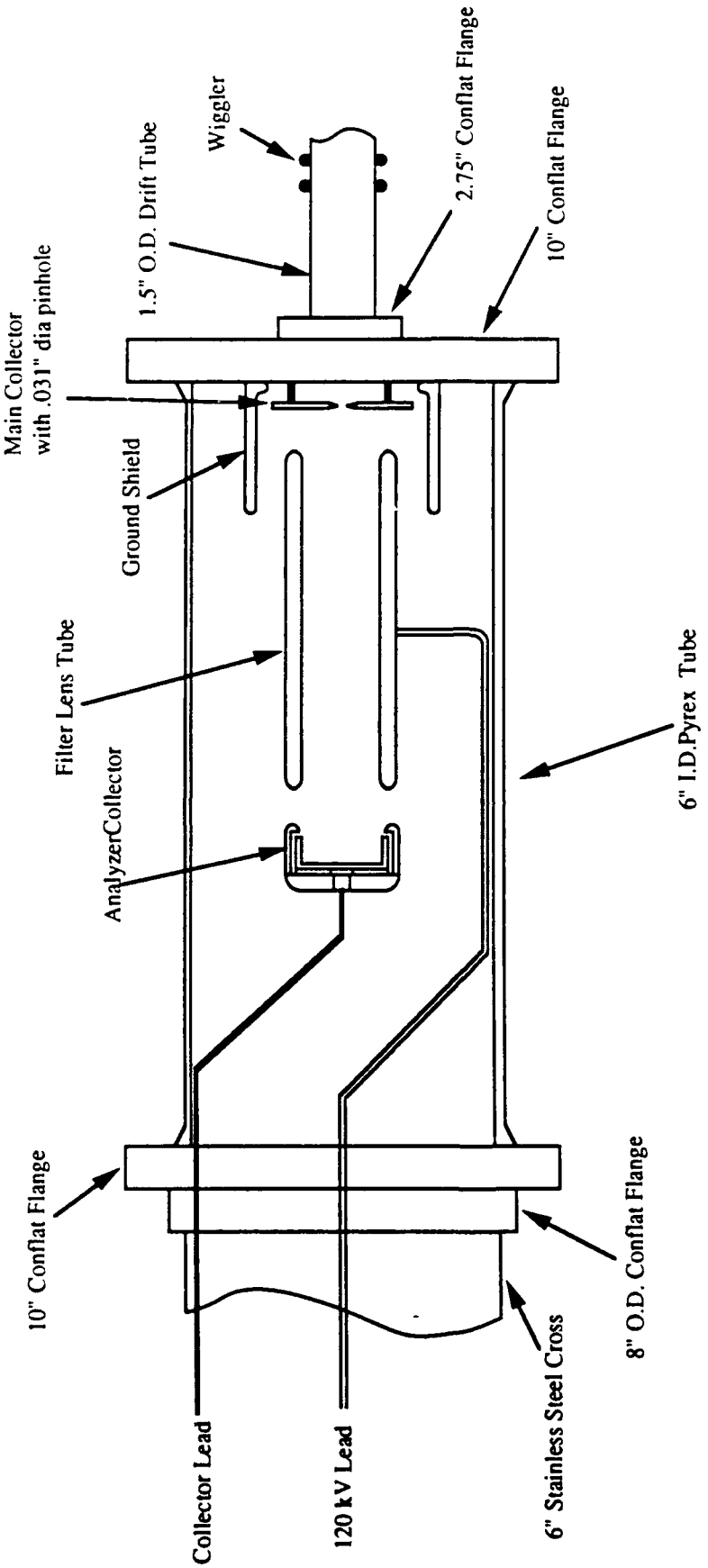

Figure 8: Details of the velocity analyzer construction. The filter lens tube diameter was made large enough to pass electrons with large gyroradii. This required enlarging the vacuum vessel with a 6-inch Pyrex glass tube.

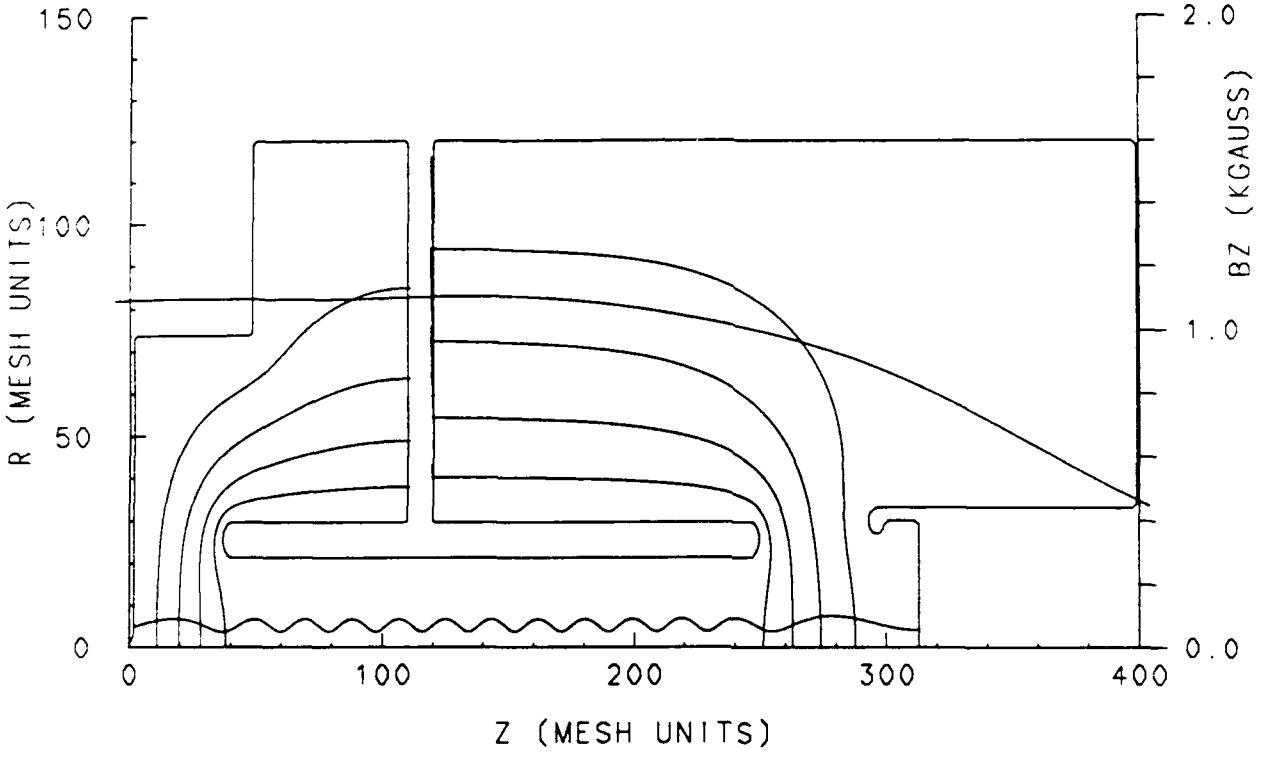

Figure 9: Trajectory of a 75-*kV* electron with $v_\perp/v_\parallel = 0.174$ and 65 *kV* negative applied to the filter lens tube. In this case, the electron has enough parallel energy to pass through the tube to the collector.

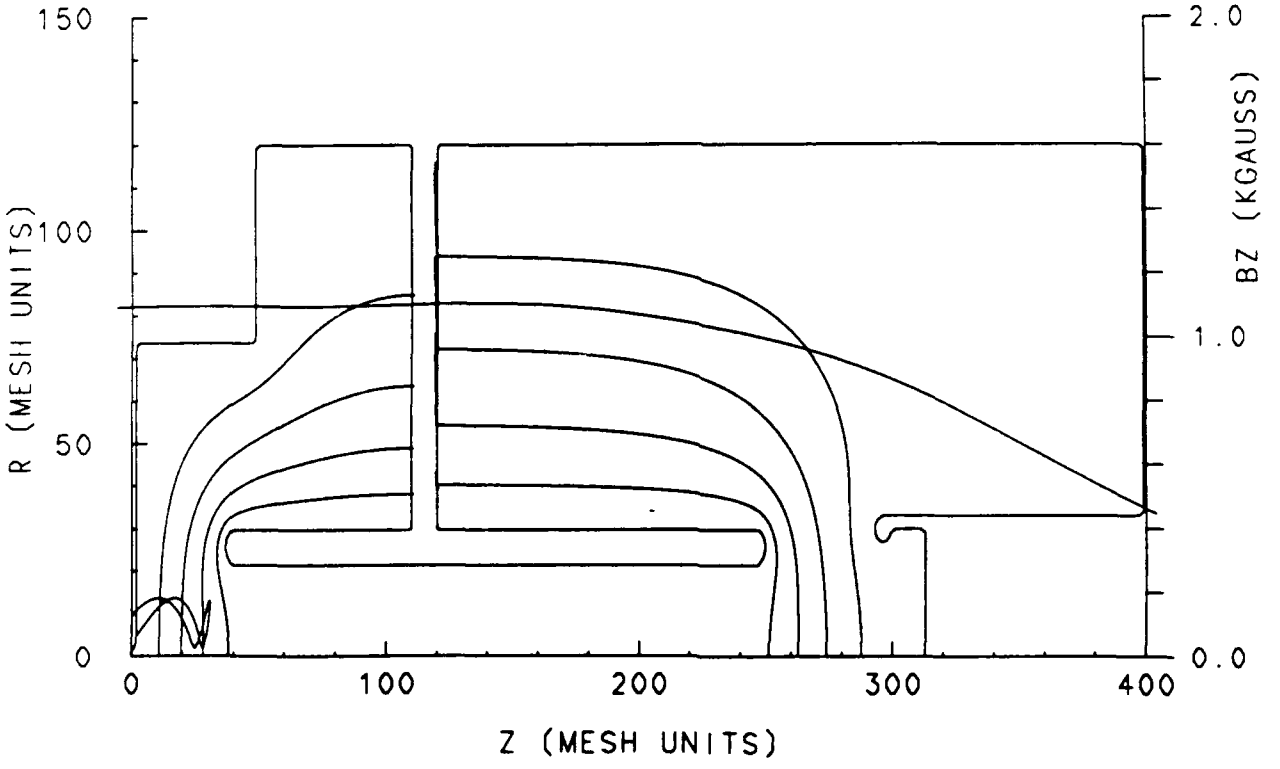

Figure 10: Same situation as in Fig. 9 except $v_\perp/v_\parallel = 0.698$. In this case, the electron is reflected back because its parallel energy is too low to overcome the potential of the filter lens tube.

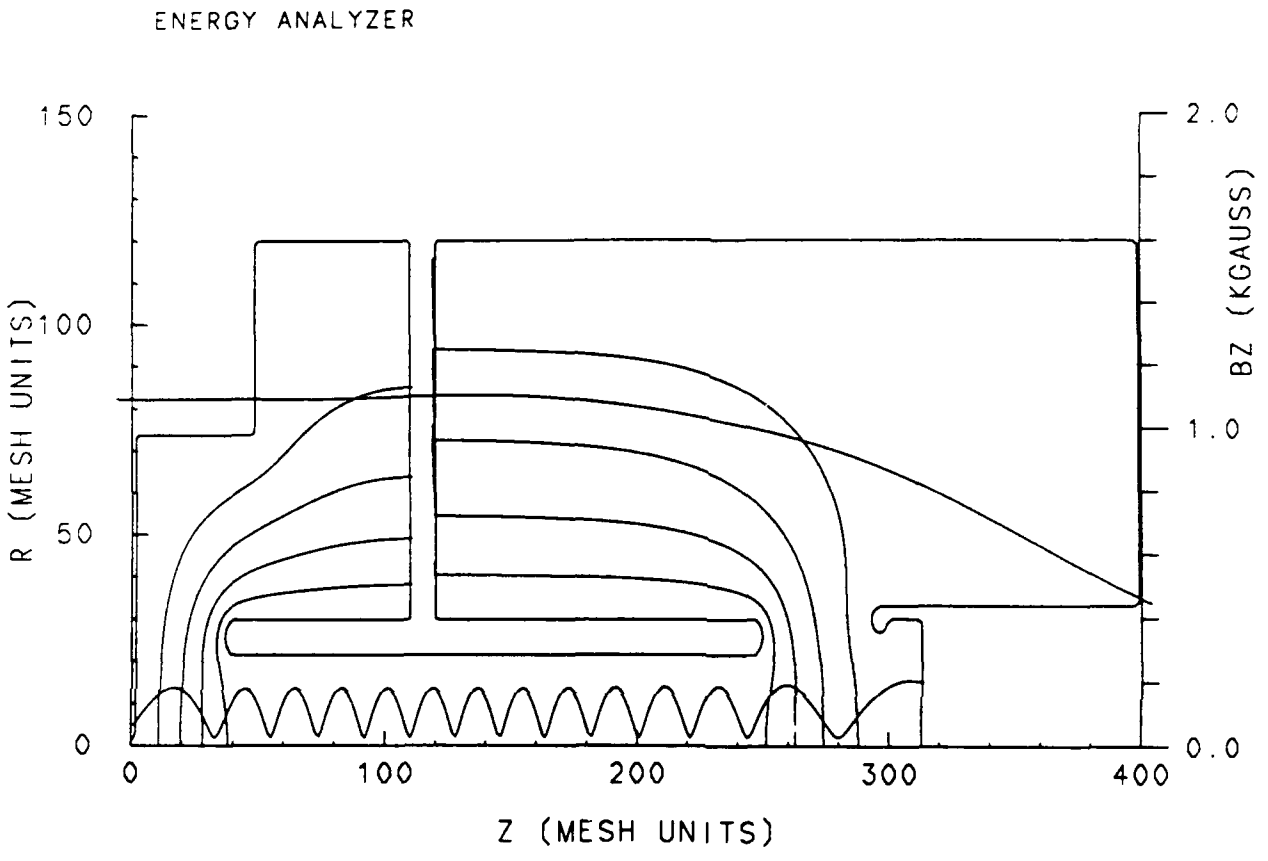

Figure 11: Same situation as in Fig. 10 except the filter lens tube potential is changed to 30 *kV* negative. In this case, the electron passes through the filter lens tube to the collector because its parallel energy is high enough to overcome the potential of the filter lens tube.

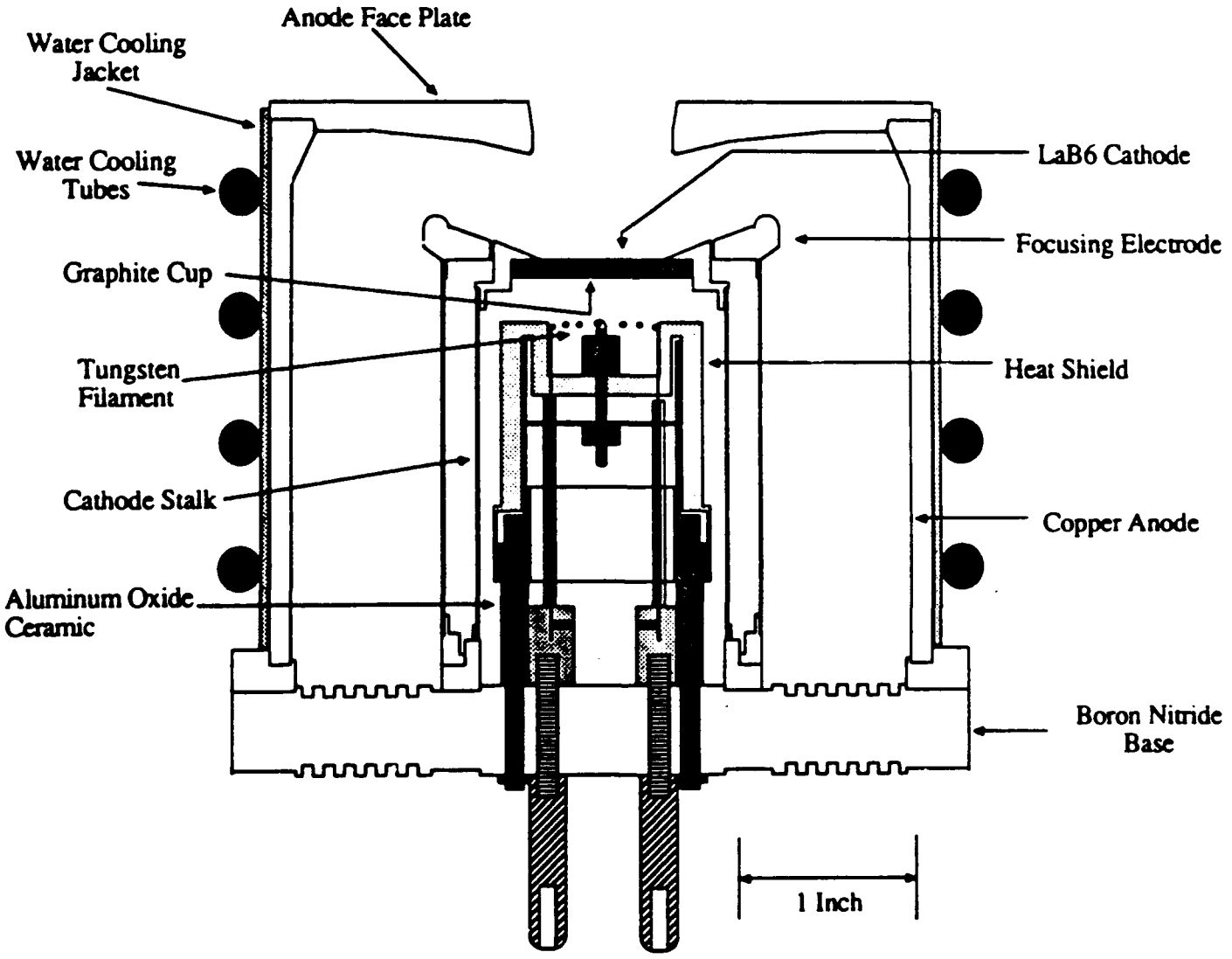

Figure 12: Electron gun with 4-inch anode diameter. Breakdown occurred across the boron nitride base between the anode and the cathode stalk.

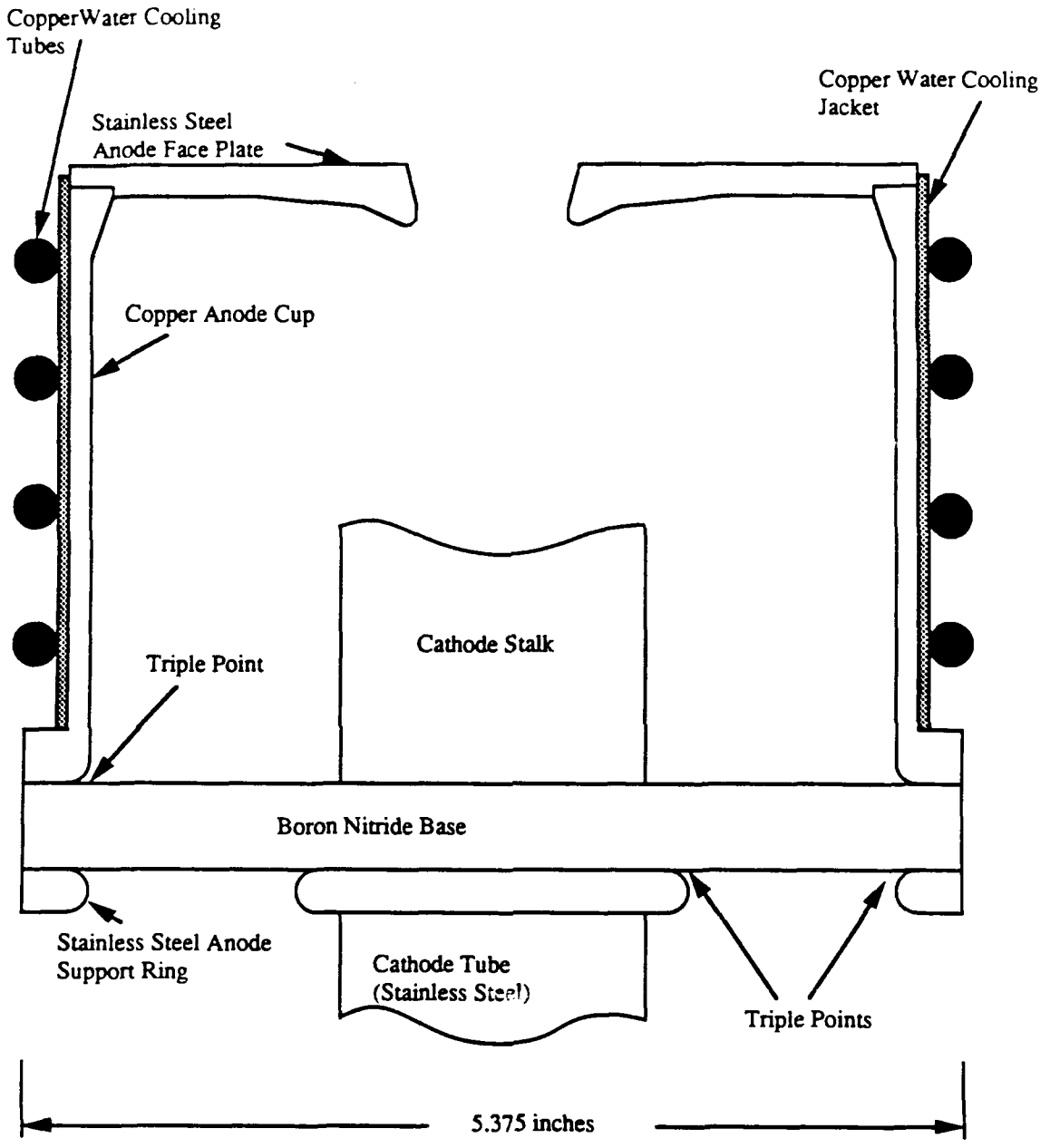

Figure 13: Electron gun with anode enlarged to 5.375 inches diameter. The boron nitride base was enlarged and grooves were cut in it with sawtooth shape.

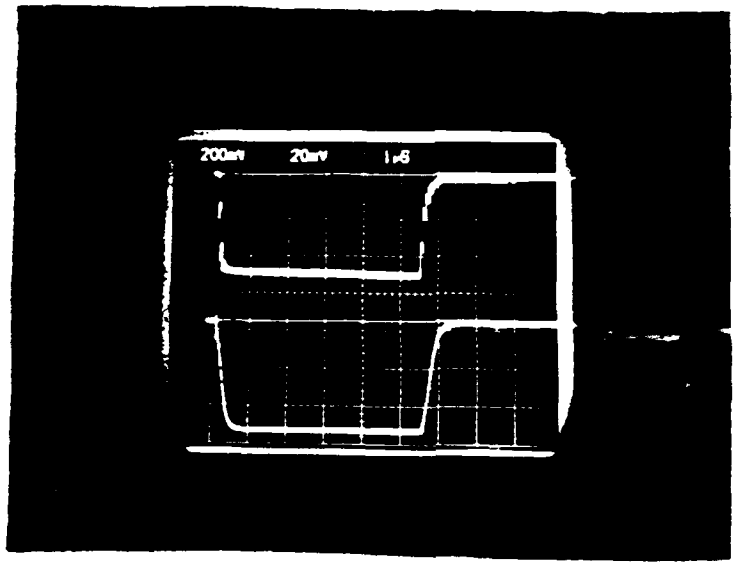

Resistive voltage divider calibration.
Top trace: Tektronix voltage probe
Lower trace: Voltage divider
Time scale: 1 µs/ div.

Figure 14 Resistive voltage divider calibration versus a Tektronix scope probe for comparison and a 500-volt pulse.

3. WIGGLER DESIGN AND TEST

During the period of this contract, the design of a wiggler was begun. The type of wiggler chosen is called a "bifurcated, bifilar" wiggler.[4,5] This type is not widely used on devices using wigglers because the winding is a little more complex, but it has the advantage that tapers in wiggler field strength are easily built into the wiggler. The method of design[5] is to specify the parameters of the desired electron orbit such as $\alpha = v_\perp/v_\parallel$ at the exit, the pitch and its taper $p(z)$, the initial velocity, and the axial field, and then solve for the required wiggler current taper.

The geometry of the wiggler is shown in Fig. 15 as a cross section of the winding. The angle $\delta(z)$ is the half angle between wires carrying opposite currents. When $\delta = 0$, the wiggler field is zero and when $\delta = 90°$, the wiggler field is maximum. Taper in the field is obtained by varying δ from 0 to 90°.

An example of the variation of δ is shown in Fig. 16. This curve is obtained from a computer program[6] which solves the design problem as specified in Ref. 5. A report on this design is included as Appendix C in this report.

The design procedure is for a specified input beam voltage, wiggler current, alpha, and guide field value. These four values are called the "design values." When conditions are changed from the design values, the electron trajectories must be found by integrating the equations of motion. This was done for a wiggler model which assumes a linear variation of $\delta(z)$ and uses a nonuniform (i.e., realizable[7]) analytical expression for the wiggler field. Variable pitch is also included. This computer program will be used to model the response of the RPA by calculating the velocity components and transverse positions of electrons as they enter the RPA, and then using the SLAC EGUN code to analyze the trajectories of those electrons that enter the RPA as they go through the RPA.

A number of cases are given in Appendix C. These include electrons that enter the wiggler on the magnetic axis with no perpendicular velocity for the design wiggler current and for 165% of the design current; and electrons that enter off the axis with no initial perpendicular velocity and

with 5% initial perpendicular energy. Two test cases are run with no wiggler current and with and without initial perpendicular energy. The results of these runs are given in Appendix C.

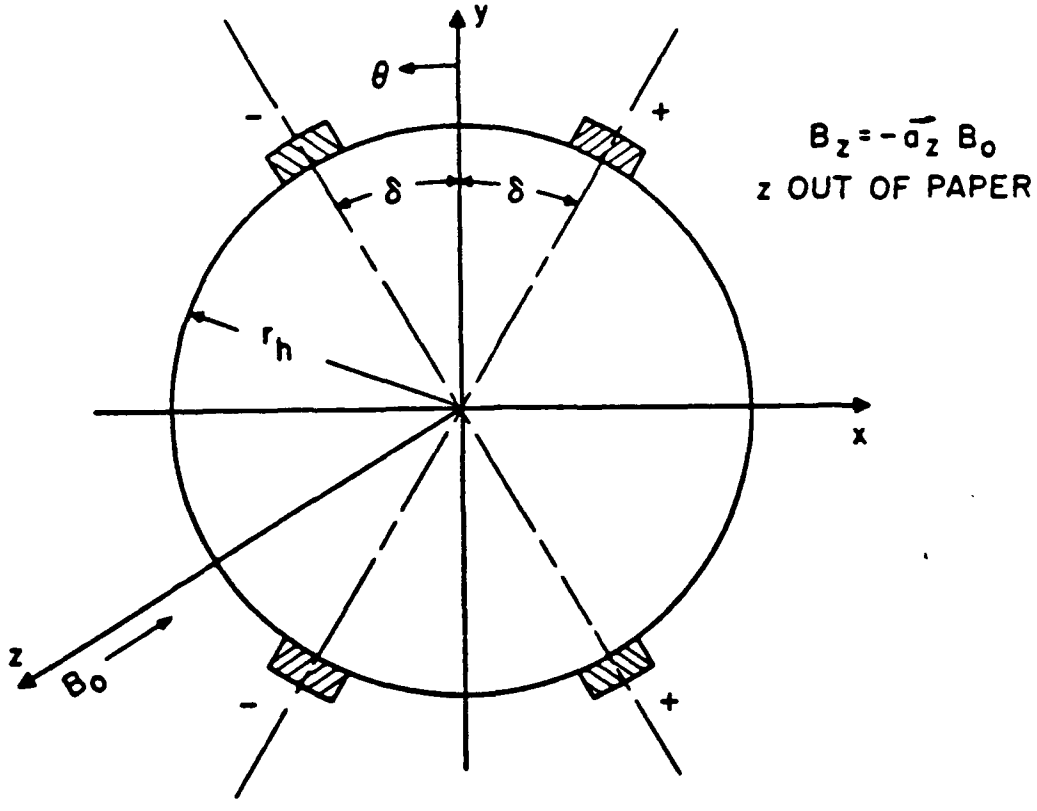

Figure 15: Illustration of how the bifurcated bifilar wiggler is wound. When $\delta = 0$, the wiggler field is zero; and when $\delta = 90°$, it has its largest value. δ is continuously varied with z to provide entrance taper for the wiggler.

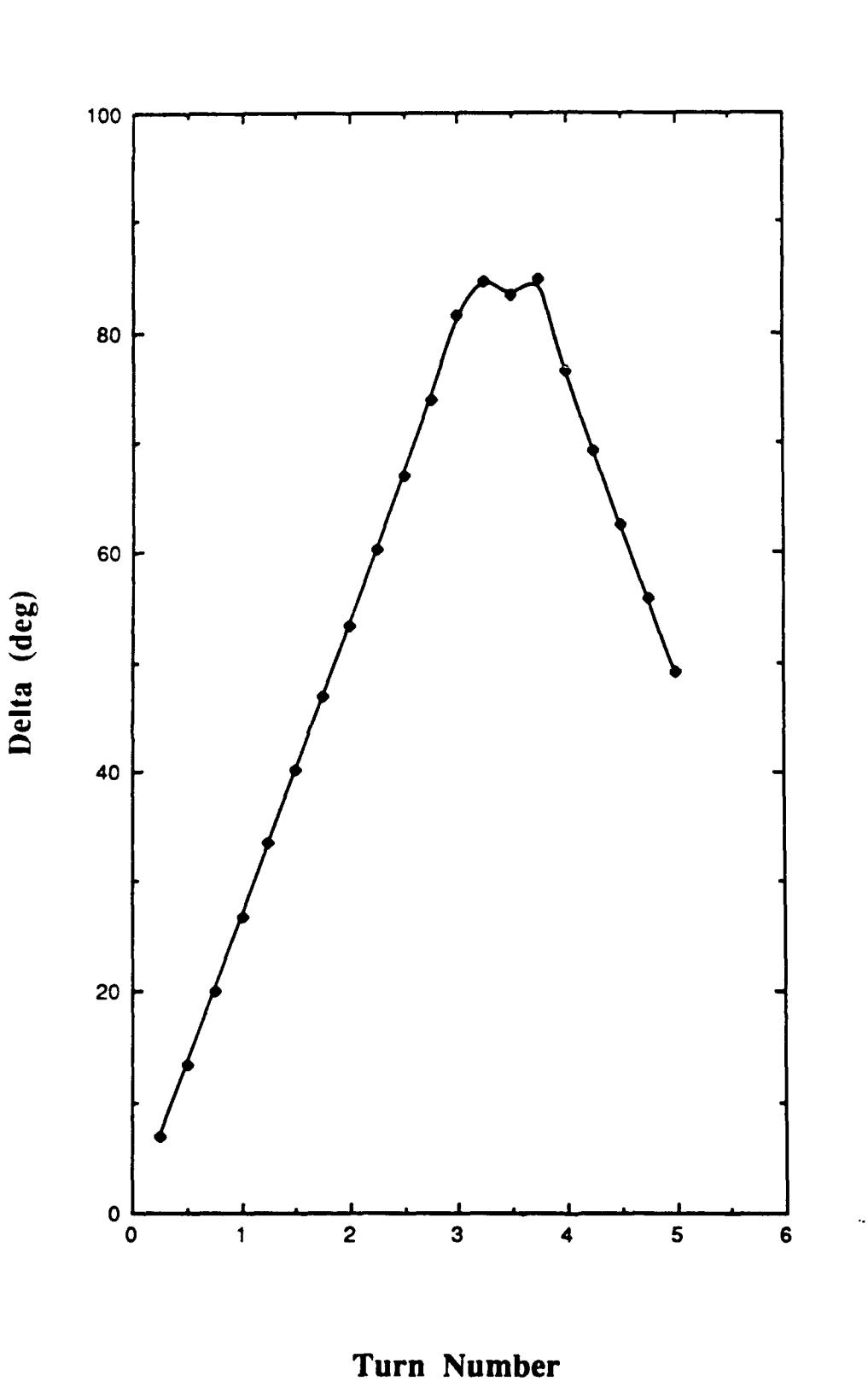

Figure 16: The variation of $\delta(z)$ obtained from the computer program. The wiggler field magnitude is proportional to sin $\delta(z)$. Turn number is proportional to z.

4. SUMMARY

The period covered by this report was primarily a rebuilding period. The Marx generator was improved by adding capacitance, the crowbar system was made operational, and the magnetic field was added. The vacuum system was changed in orientation and a pump was added.

The primary problem experienced in this period was with arcing in the electron gun. This was solved by increasing the gun diameter, but we were limited to 80-85 *kV*.

Progress was made on the design and analysis of the wiggler, calculation of trajectories through the wiggler, and analysis of the retarding potential analyzer. Safety shielding and interlocks were built.

REFERENCES

1. M. E. Herniter, "A Bombardment Heated LaB_6 Thermionic Cathode Electron Gun," Ph.D. Thesis, Department of Electrical Engineering and Computer Science, The University of Michigan, Ann Arbor, 1989.
2. W. Herrmannsfeldt, "Electron Trajectory Program," Tech. Rep. No. 226, SLAC, Stanford University, November 1979.
3. M. Caulton, "Retarding-field analyzers for the measurement of axial velocity distributions in electron beams," *RCA Review*, **26**: 217-241 (June 1965).
4. J. Fajans, "End effects of a bifilar magnetic wiggler," *J. Appl. Phys.*, **55**:43-50 (January 1, 1984).
5. R. C. Wingerson, T. H. Dupree, and D. J. Rose, *Phys. Fluids*, **7**:1475 (1964).
6. A. Singh, "Generation and Wave Propagation Characteristics of Spiraling Electron Beams," Ph.D. Thesis, Department of Electrical Engineering and Computer Science, The University of Michigan, Ann Arbor, 1972.
7. P. Diament, "Electron orbits and stability in realizable and unrealizable wigglers of free-electron lasers," *Phys. Rev. A*, **23**:2537-2552 (May 1981).

APPENDIX A

Pulsed Cathode Heating Method

GEORGE A. LIPSCOMB, MEMBER, IEEE, MARC E. HERNITER, MEMBER, IEEE, AND WARD D. GETTY, MEMBER, IEEE

Abstract—One drawback in the use of lanthanum hexaboride thermionic cathodes at high current density is the amount of steady-state heating power needed to heat the cathode to the desired temperature range (≈ 1800°C). With continuous heating, approximately 1000 W of power are required to keep a 1-in diam cathode at 1800°C. For 2-in diam cathodes, the power requirement rises to 3 to 5 kW. Cathode evaporation is significant with continuous heating at 1800°C. To reduce the average power requirement and evaporation in pulsed experiments, a transient heating scheme has been investigated which allows single shot or slow, cyclic heating of the cathode. This scheme gives a few seconds of peak temperature during which many microsecond-length beam pulses can be fired with a suitable pulse modulator. For a 1-in diam cathode heated at a 120-s repetition period, the average power requirement drops by over an order of magnitude. This scheme provides average power reduction for larger cathodes to the same extent, and simplifies the voltage isolation problem in supplying cathode heating power. In this paper we present calculations based on a thermal model with electron bombardment heating, and compare these calculations with a pulsed-heating experiment.

I. INTRODUCTION

FREE-ELECTRON Lasers (FEL's) have employed a variety of cathodes in their electron beam sources. Cathodes in use or under development for FEL's include lanthanum hexaboride (LaB_6) thermionic cathodes [1], [2], cold field-emission cathodes [3], thermionic dispenser cathodes [4], plasma cathodes [5], and metal photocathodes [6]. In the present research a thermionic cathode of LaB_6 has been developed for high current density operation in a Pierce-type electron gun [1], [7]. An objective of the development has been to heat the cathode to 1800°C, the temperature where the Richardson–Dushman equation predicts that 40 A/cm^2 emission current should be obtained. The electron gun has a perveance of 3.2×10^{-6} A/V$^{3/2}$ and has been constructed with a 1-in diam LaB_6 cathode for operation up to 120 kV. The achieved cathode temperature range was 1650°–1800°C.

The use of a thermionic cathode in a relativistic electron-beam machine would be a great advantage over plasma cathodes for long beam pulses because there would be no anode–cathode gap closure problem. In order to reduce the average cathode heating power, we have analyzed and tested a pulsed heating scheme for a LaB_6 cathode which is suitable for the cyclic or single-shot pulsed operation of an electron gun in a FEL, CARM (Cyclotron Autoresonance Maser), or similar device requiring a high cathode current density and relativistic beam energies. The method greatly reduces the average cathode heating power and uses a relatively simple electrical heating circuit. It is suitable for very high-voltage electron guns because the problem of isolating the cathode heating supply is simplified.

A. Continuous-Mode Cathode Heating

Steady-state cathode heating [1], [7] is done by continuous electron bombardment of the LaB_6 cathode from a temperature-limited tungsten filament. Temperature-limited electron bombardment heating is open-loop unstable [7] and requires a control circuit to eliminate the instability [1], [7]. Bombardment and filament power is supplied to the electron gun through an inductive isolation system. This system uses three 120-kV isolation inductors that are large enough to prevent damaging current from flowing through the control circuit during the high-voltage electron-gun pulse. A 4-stage Marx generator is used to drive the gun cathode approximately 120 kV negative to produce the main beam pulse.

Steady-state heating results [1], [7] show that the 1-in cathode requires up to 1050 W of heating power to heat it to 1800°C. The electron-gun anode is water cooled, and cooling fans are used on the vacuum system near the gun region. There is significant evaporation from the LaB_6 cathode which affects the bombardment heating system by activating the tungsten filament. If a 2-in diam cathode is used [2], the measured total heating requirement is 3 to 4 kW and it becomes more difficult to handle the heat load. In single-shot or low duty-cycle systems, it is possible to significantly reduce the average cathode heating power by pulsed heating.

B. Pulsed-Mode Cathode Heating

A theoretical and experimental study has been performed on a method for drastically reducing the average power requirement for heating a LaB_6 cathode to 1800°C. The method also eliminates the need for inductive isolation and heating control which are required for continuous heating. The reduced average heating power and cathode temperature lower the vacuum vessel temperature and reduce outgassing and cathode evaporation.

The pulsed-mode heating method reduces the heat load by an order of magnitude and is suitable for very high voltage operation of a thermionic cathode electron gun. It

Manuscript received June 15, 1989; revised August 15, 1989. This work was supported by the Office of Naval Research.

G. A. Lipscomb was with the Department of Electrical Engineering and Computer Science, University of Michigan, Ann Arbor, MI 48109. He is now with the U.S. Naval Jet Pilot School, Meridian, MS 39305.

M. E. Herniter was with the Department of Electrical Engineering and Computer Science, University of Michigan, Ann Arbor, MI 48109. He is now with the Department of Electrical Engineering, Wichita State University, Wichita, KS 67208.

W. D. Getty is with the Department of Electrical Engineering and Computer Science, University of Michigan, Ann Arbor, MI 48109.

IEEE Log Number 8931374.

0093-3813/89/1200-0898$01.00

APPENDIX B

Abstract Submitted for the Thirty-first Annual Meeting
Division of Plasma Physics
November 13-17 1989

Category Number and Subject 4.19
__ Theory _x Experiment

Transport of a 120-kV, 100-A Electron Beam From a LaB_6 Cathode Through Combined Wiggler and Axial Magnetic Fields. K. D. PEARCE and W.D. GETTY, Univ. of Michigan.*-- An electron beam is produced by a 4-stage, crowbarred Marx generator with a 5-μs, 120-kV, 100-A square output pulse with a risetime of less than 1 μs. The electron gun contains a lanthanum hexaboride (LaB_6) cathode which is heated by electron bombardment and can produce a current density of 30 A/cm^2 in a Pierce electron-gun geometry. The cathode is immersed in a collimating axial magnetic field of 0.17 T which extends over the entire length of the beam. The electromagnet bifilar wiggler has a period of ≈ 2.7 cm and is 10 wavelengths long. The beam is transported to a collector ≈ 5 cm beyond the wiggler. Diagnostics consist of a Rogowski coil, capacitive probes, a capacitive-divider beam voltage monitor, and a transformer beam-current monitor. An electron retarding potential energy analyzer is under development for a study of the effect of the wiggler on the beam velocity distribution function.
* Work supported by the Office of Naval Research.

_x Prefer Poster Session
__ Prefer Oral Session
__ No Preference
__ This poster/oral should be placed in the following grouping: (specify order)
_____
_____
__ Special Facilities Requested (e.g., movie projector)
_____
_____
__ Other Special Requests
_____
_____

Submitted by:

_____
(Signature of APS Member)

Ward D. Getty
(Same Name Typewritten)

Dept. of Elec. Eng. & Comp. Sci.
1124 EECS Building
University of Michigan
Ann Arbor, MI 48109-2122
(Address)

This form, or a reasonable facsimile, plus **TWO XEROX COPIES**, must be received by **NO LATER THAN NOON**, Monday, July 10, 1989 at the following address:

Saralyn Stewart
Institute for Fusion Studies
RLM 11.234
The University of Texas at Austin
Austin, TX 78712
Telephone: (512) 471-4378

APPENDIX C

Design, Construction, and Analysis of an Electromagnetic Bifilar Wiggler

Ron R. Temske

N.E. 799
Final Report

Advisor:
Dr. Ward Getty

University of Michigan
1990

Introduction

This paper details the design, construction, and analysis of an electromagnetic, bifilar wiggler for use on the SUREFIRE experiment (System Undulator Radiation Experiment of Free Intense Relativistic Electrons). The SUREFIRE experiment currently operates at 75 kV, with 5 μs pulses. The beam current is typically 20 Amps, and the thermionic cathode heating power varies between 300 to 800 Watts. The entire beam path is immersed in an 1100 Gauss axial magnetic field.

There are four different stages of the wiggler development which will be discussed. The first step involves the computer aided design of the wiggler itself. A computer program, written in FORTRAN on the MTS computing system, was developed to calculate the physical layout of the wiggler. As the name bifilar implies, the wiggler is physically made up of two sets of magnet wire, wound in a helical pattern. The MTS program calculates the physical positioning of these wires based on input design parameters. Upon successful calculation, the program produces a 1 : 1 scale plot which can be used to construct the wiggler.

The second stage is the actual construction of the wiggler itself. The plot, which was produced in stage one, is wrapped around a stainless steel tube, 30 cm long. Two sets of 14 AWG enamel magnet wire are wrapped around the tube, following the pattern on the plot. The wires are held in place by fiberglass cloth tape.

The third stage involved measuring the magnetic field produced by the wiggler, and comparing this field to the theoretically predicted fields from stage one.

Finally, the fourth stage consisted of the development of a computer program to analyze the electrons motion through the wiggler. This program solves the particle equations of motion for the electron beam, and can accommodate a number of input parameters, including a variable guiding center and variable initial perpendicular energy.

II. Wiggler Design

In the design of the wiggler, there are a number of physical constraints that have to be considered. Due to the hardware layout of SUREFIRE, we need a wiggler that is 30 cm long and 3.8 cm in diameter. The axial magnetic field of the system is 1100 gauss, and this also has to be considered.

A very important consideration is the current needed to drive the wiggler. We want the wiggler to require less than 200 amps to operate if possible. The reasons for this are that a 200 amp power supply is relatively easy to build, and if there is too much current running through the wiggler, there is a substantial risk of the wiggler physically ripping apart from the strong magnetic field.

The real challenge results from the fact that we want to maintain an acceptable windup ratio (defined as the perpendicular velocity of the electron at the exit of the wiggler divided by the parallel velocity at the entrance of the wiggler. Our goal is a windup ratio > 0.7) while satisfying all the above criteria. There are three ways to increase the windup ratio of a wiggler. The easiest method is to increase the driving current, but as mentioned above, we wanted to stay below 200 amps if possible. The second way is to increase the length of the wiggler, but this also is not possible in our system. Finally, you can increase the windup ratio for a fixed current and length, by increasing the number of turns of wire on the wiggler. Figure 2.1 shows the relationship between the wiggler current, the windup ratio, and the number of turns, N.

With the above parameters, we were able to design a wiggler that will produce a windup ratio of 0.8316 with 7 turns and a driving current of only 152 amps.

To aid in the construction of the wiggler, the computer program was designed to make a scale plot of the wiggler, with lines representing the physical positioning of the wires. A copy of this plot is included as figure 2.2. Please see Appendix A for an in-depth review of the mechanics of this computer program.

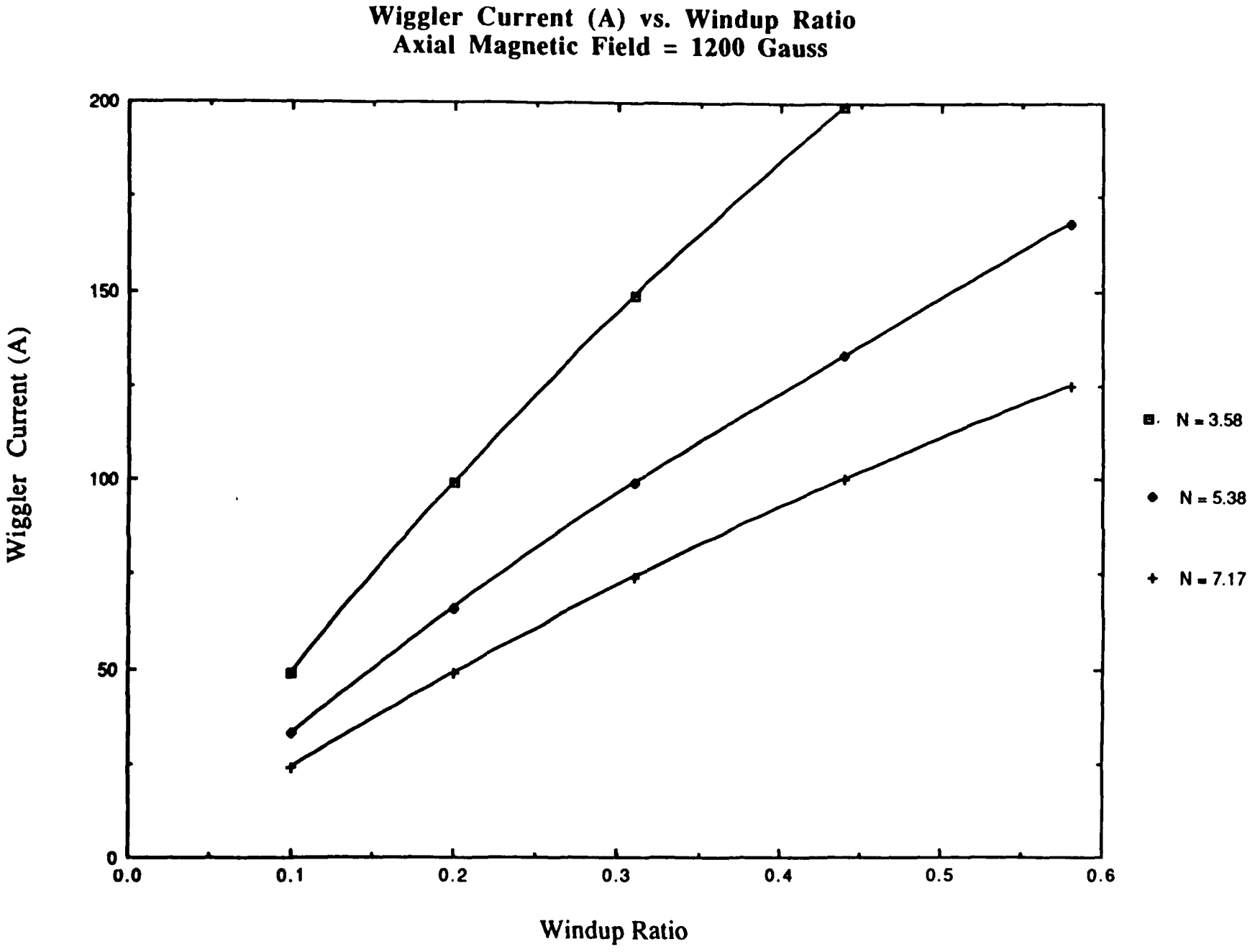
Wiggler Current (A) vs. Windup Ratio
Axial Magnetic Field = 1200 Gauss
Wiggler Current (A)
200
150
100
50
0
0.0
0.1
0.2
0.3
0.4
0.5
0.6
Windup Ratio
N = 3.58
N = 5.38
N = 7.17

Figure 2.1

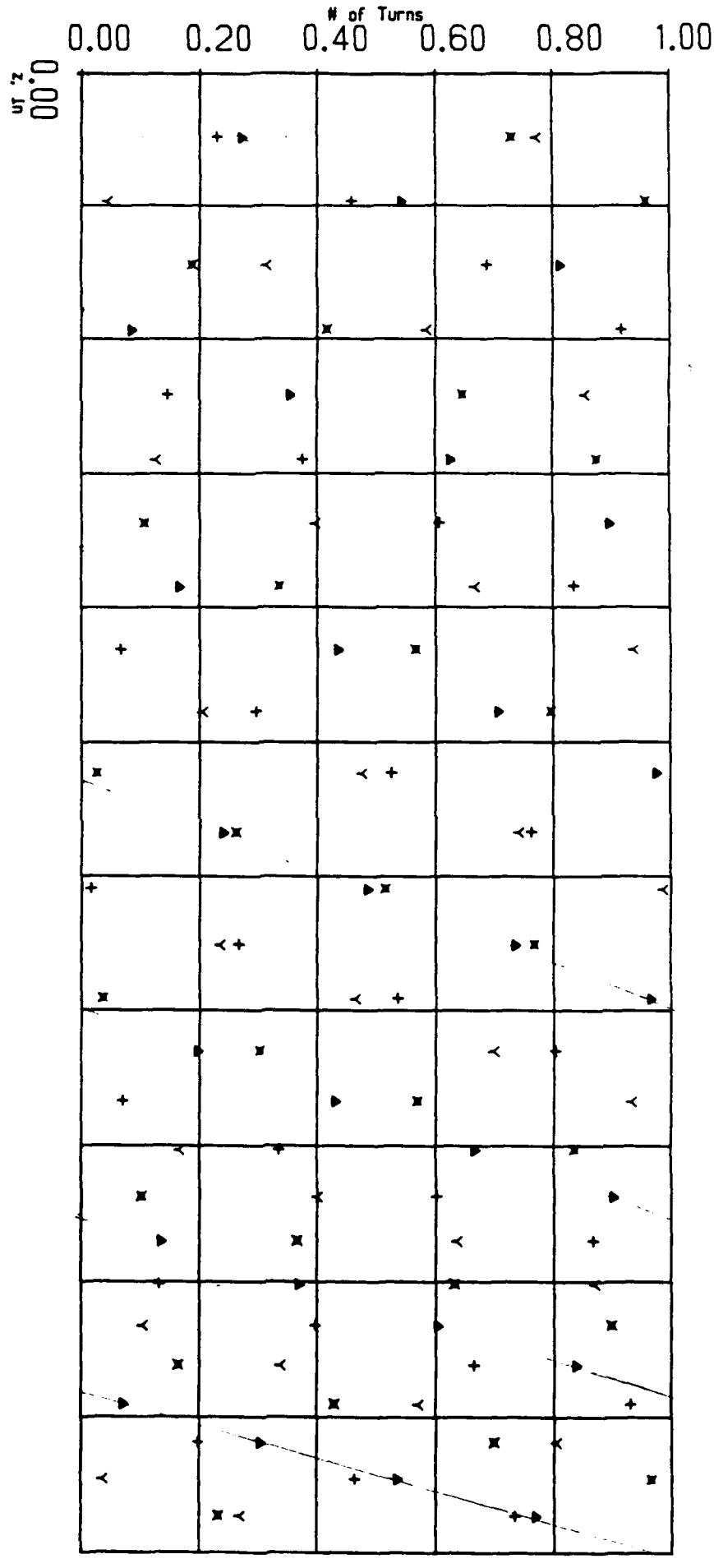

Figure 2-2

III. Construction of the Wiggler

The wiggler is built on a 30 cm long, 3.8 cm diameter stainless steel tube. A thin (1mm thick) piece of mylar is epoxied to the outside of the tube to prevent any possible shorting of the wires to the tube. The plot generated in part II (figure 2.2), is then attached to the mylar on the tube. Two sets of 14 AWG wire are wound around the tube following the pattern laid out on the plot. These wires are held in place by layers of fiberglass cloth tape.

IV. Measurement of the Magnetic Field

Once the wiggler was constructed, we wanted to measure the magnetic field produced to see if it matched well with theory before attaching the wiggler to the SUREFIRE system. The magnetic field was measured using a transverse probe connected to a gaussmeter. The field was measured at a current of 8 amps. Figure 4.1 shows the measured transverse magnetic field produced by the wiggler vs. the axial position inside the wiggler. This graph has been normalized to 152 amps for ease of comparison to theory.

Figure 4.2 shows the theoretical transverse magnetic field produced by the wiggler vs. the axial position inside the wiggler.

The two graphs match well in the relative amplitude of the peaks. The graphs are somewhat out of phase, but this is to be expected, as the theoretical plot is given with respect to the y-axis of the wiggler. Since this axis is arbitrary, there is no good way to measure the field in the same phase as the program calculates. It is the relative amplitudes and spacing that concern us, and these match up very well.

Once we were confident that the wiggler was producing the desired magnetic field, it was attached to the SUREFIRE system. The final (and most involved) stage of the project consists of determining the electron trajectories through the wiggler. This will be discussed in chapter 5.

B-Field vs. Position in Wiggler
For 152 Amp Driving Current
(Experimental)

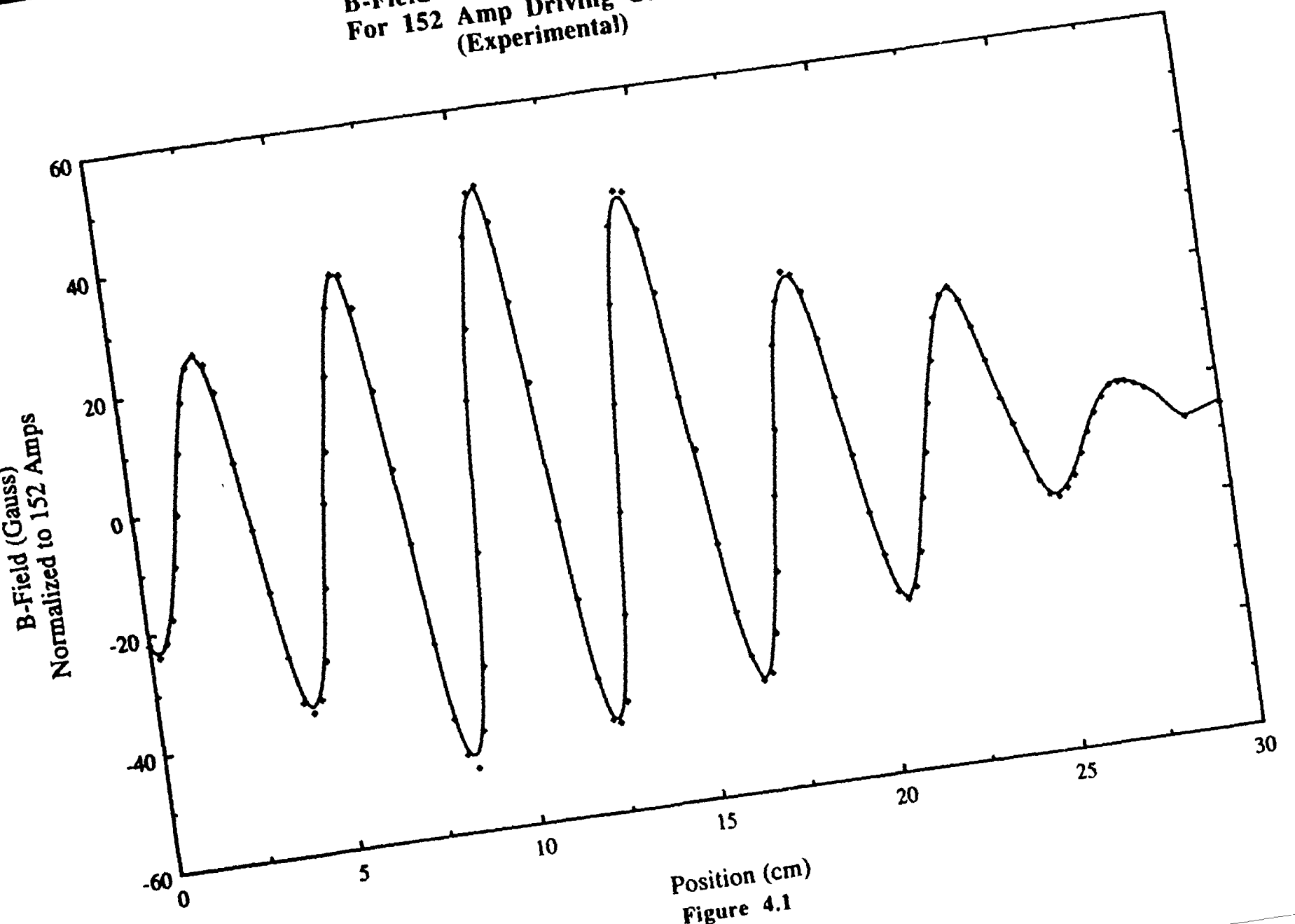

Figure 4.1

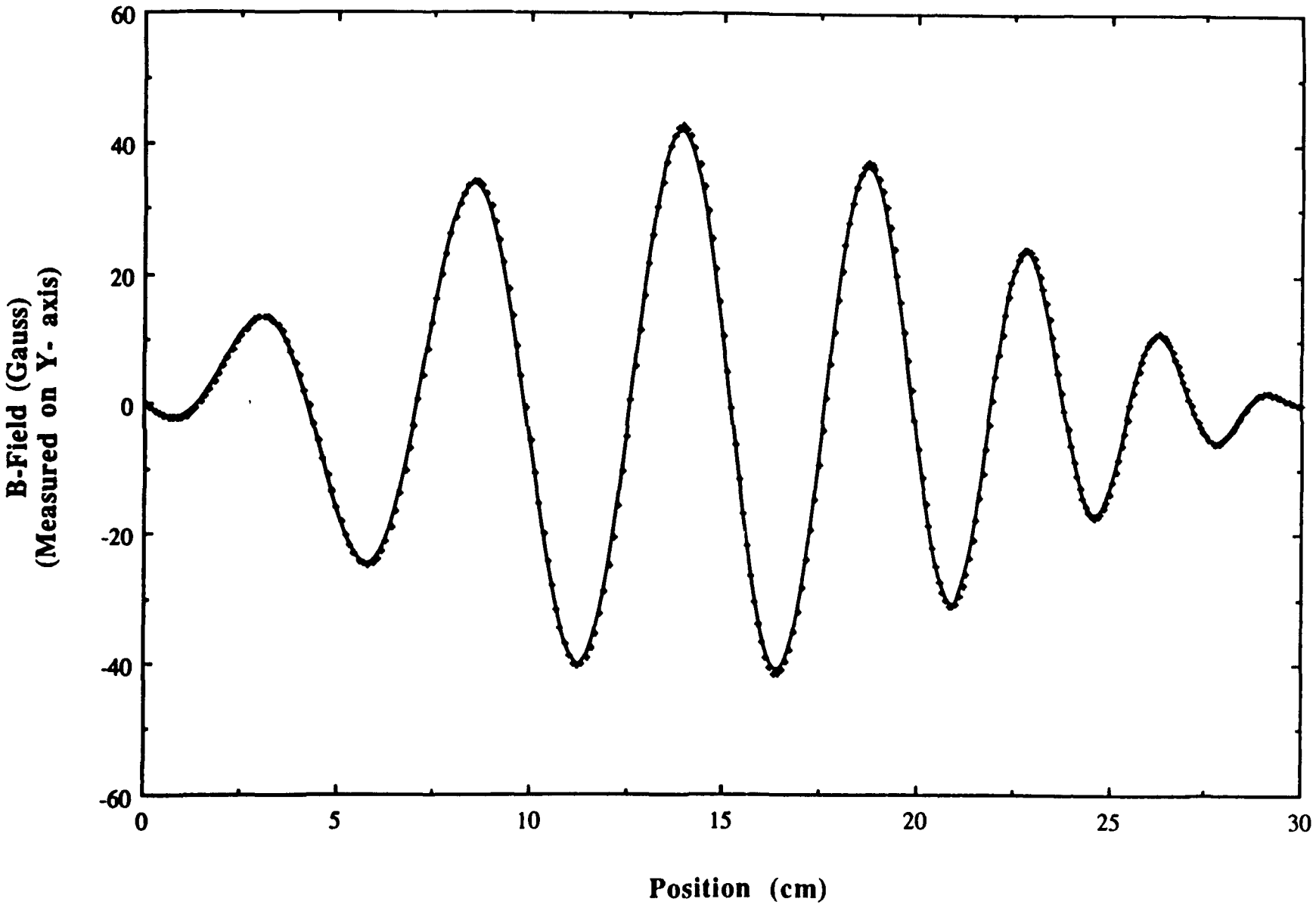
B-Field vs. Position in Wiggler
For 152 Amp Driving Current
(Theoretical)
B-Field (Gauss)
(Measured on Y- axis)
60
40
20
0
-20
-40
-60
0
5
10
15
20
25
30
Position (cm)

Figure 4.2

V. Calculation of Electron Trajectories

The final, and most involved, phase of the project was the analysis of an electrons motion through the wiggler. A computer program was developed for this task. The program looks at single particle motion through the wiggler, and any space charge effects are neglected. This is an acceptable approximation for the SUREFIRE parameters.

The main purpose of the program is to solve the equations of motion of an electron in a magnetic field :

$$\frac{dVx}{dt} = \frac{-e}{m_o\gamma}(V_yB_z - V_zB_y) \qquad (1)$$

$$\frac{dVy}{dt} = \frac{-e}{m_o\gamma}(V_zB_x - V_xB_z) \qquad (2)$$

$$\frac{dVz}{dt} = \frac{-e}{m_o\gamma}(V_xB_y - V_yB_x) \qquad (3)$$

$$\frac{dX}{dt} = V_x \qquad (4)$$

$$\frac{dY}{dt} = V_y \qquad (5)$$

$$\frac{dZ}{dt} = V_z \qquad (6)$$

Where,

m_o is the rest mass of the electron

$$\gamma = \frac{1}{\sqrt{(1 - \frac{v^2}{c^2})}}$$

The equations for the magnetic field produced by the wiggler are :

$$Bx = \beta 1[I0(\rho)\sin(\Phi) + I2(\rho)\sin(2X + \Phi)]$$

$$By = \beta 1[I0(\rho)\cos(\Phi) + I2(\rho)\cos(2X + \Phi)]$$

$$Bz = 2\beta 1 I1(\rho)\sin(X)$$

$$X = \int 2\pi dz / p(z) - \theta = \theta - \Phi$$

Where Theta and Phi are as defined in figure 5.0.

And rho is defined :

$$\rho = \frac{2\pi r}{P_z} = \sqrt{\frac{B_z^2 e^2 (x^2 + y^2)}{V_o^2 m^2 (1 - \xi^2 \sin^4(zn))}}$$

where
V_O is the electron energy,
zn is the fraction of length traversed (i.e. Z/Length of wiggler)
ξ is the windup ratio of the wiggler

$$Pz = Po\sqrt{1 - \sin^4(zn)\xi^2}$$

and P_o, the initial pitch is defined as

$$Po = \frac{2\pi Vom}{B_z e}$$

The constant ß1 is defined :

$$\beta 1 = \frac{\mu o I \rho h K_1'(\rho h)\sin(\delta)}{Pz}$$

where

μ_o = Permeability of free space = $4\pi * 10^{-7}$

I = Helix current in amps

δ = $zn * \pi$

I_0, I_1, I_2, and K_1' are modified Bessel functions

$$\rho h = \frac{2\pi Rh}{P_z}$$

R_h = radius of the wiggler

The computer program uses a finite difference scheme, whose algorithm is given below, to evaluate the above equations (1) - (6).

$$V_x\Big|_{t=to+\Delta t} = \left(V_x + \frac{dV_x}{dt}\Delta t + \frac{1}{2}\frac{d^2V_x}{dt^2}\Delta t^2\right)\Big|_{t=tc}$$

$$X\Big|_{t=to+\Delta t} = \left(X + V_x\Delta t + \frac{1}{2}\frac{dV_x}{dt}\Delta t^2 + \frac{1}{6}\frac{d^2V_x}{dt^2}\Delta t^3\right)\Big|_{t=tc}$$

(Similiar equations hold for Vy, Y, Vz, and Z)

The program calculates the electrons velocity and position as a function of time based on the following input parameters :

RHELIX	=	Radius of wiggler
ELCM	=	Length of wiggler in cm.
HELIXI	=	Wiggler current in Amps
EO	=	Electron energy in eV
CHIO	=	Initial phase angle of electron
GI	=	Design windup ratio
XGC, YGC	=	Coordinates of electron guiding center
PEO	=	Percentage of initial energy that is perpendicular to the z-axis

Co-ordinate System

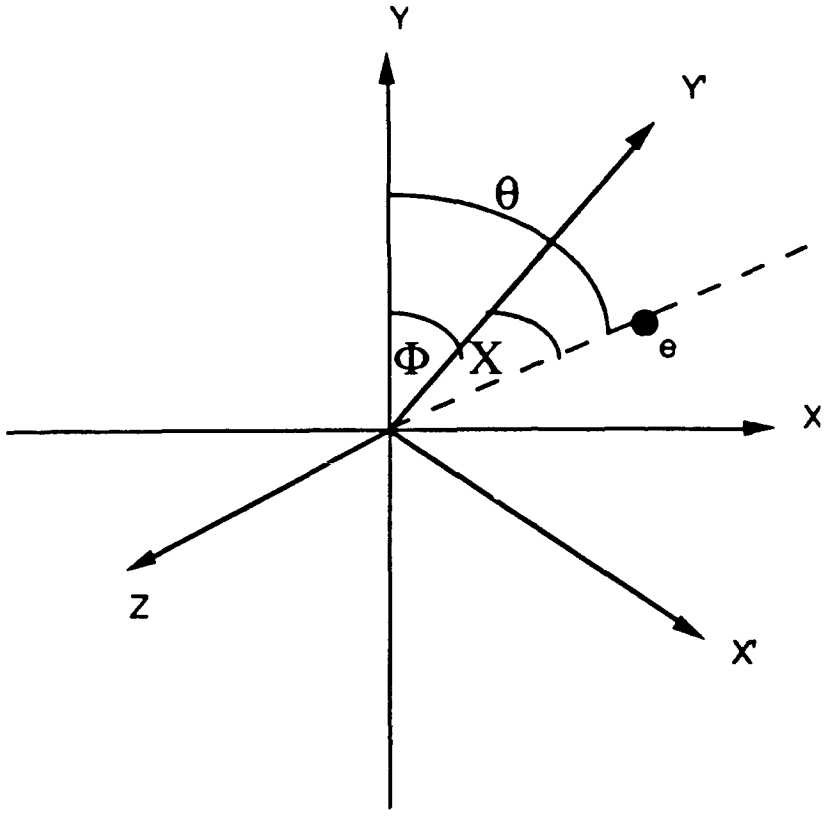

Y' Alligned with maximum transverse magnetic field

Synchronism implies

$$X = 0$$

$$\theta = \Phi$$

Figure 5.0

There are a few different ways that the output of the program can be analyzed. Figure 5.1 is an end-on view of the wiggler. The graph shows the helical motion of the electron as it traverses down the tube. Another interesting quantity to examine is the velocity of the electron as a function of the distance down the wiggler. Figure 5.2 shows Vx, Vy, Vz, and Vtotal as a function of z. Since this plot assumes no initial perpendicular energy, Vz and Vtotal are initially equal. As the electron traverses down the wiggler, the parallel energy is converted into transverse energy. Total energy of the system is conserved however, as evidenced by the value Vtotal, which remains constant at all times. Figure 5.3 shows the effects of over-driving the wiggler. The electron gains energy too quickly and becomes out of phase with the wiggler. This is evidenced by the rapid increase in Vx and Vy, followed by a slight decrease in the velocity as the electron gradually becomes in phase again.

Figure 5.4 illustrates the effects of injecting an electron off axis. The wiggler contribution to the axial magnetic field increases away from the axis, therefore an electron off axis sees a rotation in its guiding center. Figure 5.5 shows the slight instability this produces, as evidenced by the oscillation of the velocity.

In figure 5.6, the electron is injected off axis with 5 percent initial perpendicular energy. This initial perpendicular velocity makes the condition for synchronism difficult to achieve. This is evidenced in figure 5.7, where the total perpendicular velocity achieved in the wiggler is less than the other cases, even though the electron starts with some perpendicular energy.

Finally, to check the validity of the computer program, a couple of test cases were run. Case 1 (figure 5.8) involved injecting an electron off axis with no initial perpendicular energy. In this case (and in case 2), the wiggler current is input as zero, so that the only magnetic field present is a constant 1100 gauss axial field. The computer program predicts the correct electron behaviour, which is a straight shot through the tube. In figure 5.9, the electron is now injected with 5 percent initial perpendicular energy. In this case, the electron also exhibits the expected behaviour, which is a spiraling orbit, with a constant radius equal to the cyclotron radius.

X vs. Y for 152 Amps
Initial Position = (0,0)
No Initial Perpendicular Energy

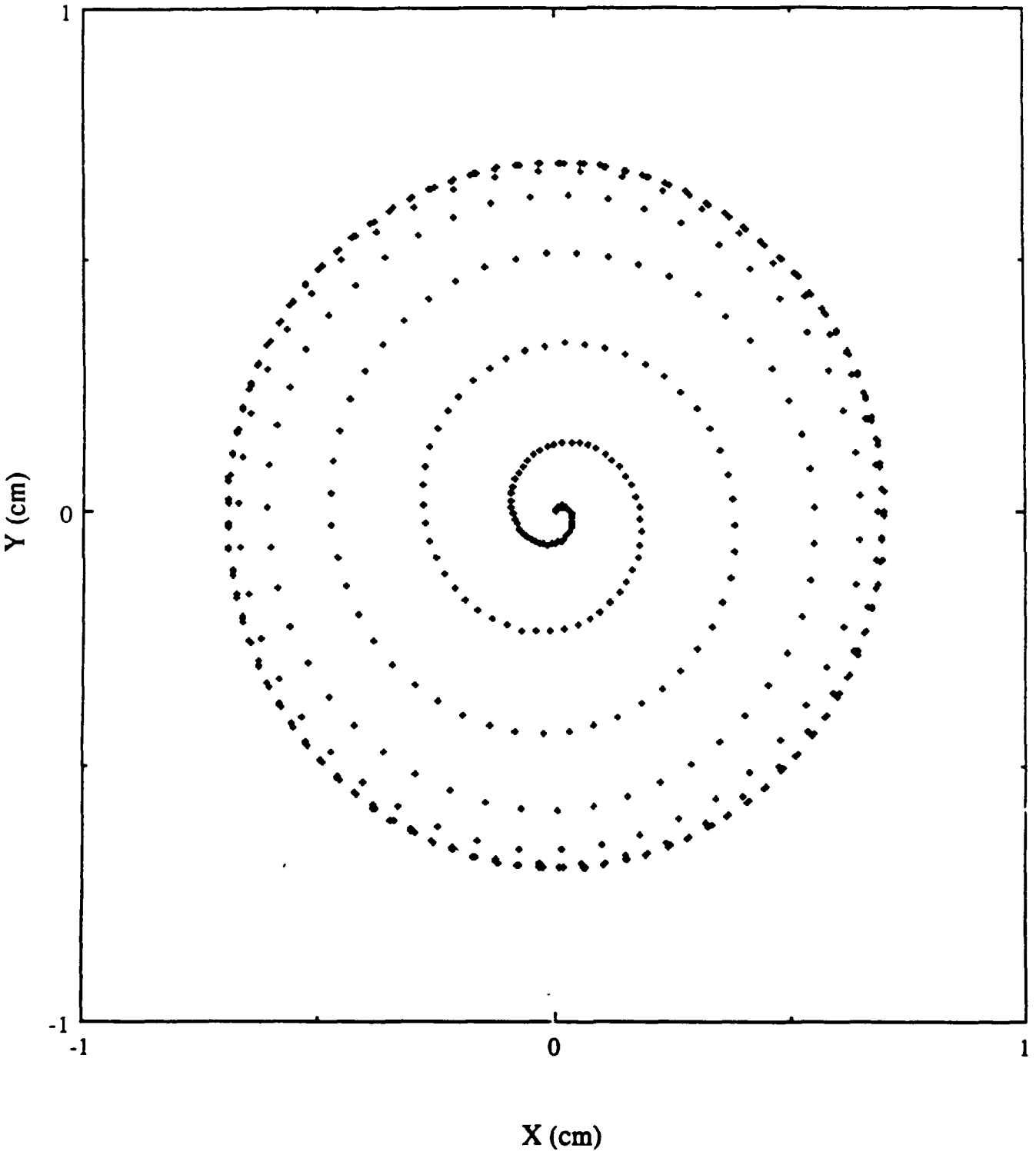

Figure 5.1

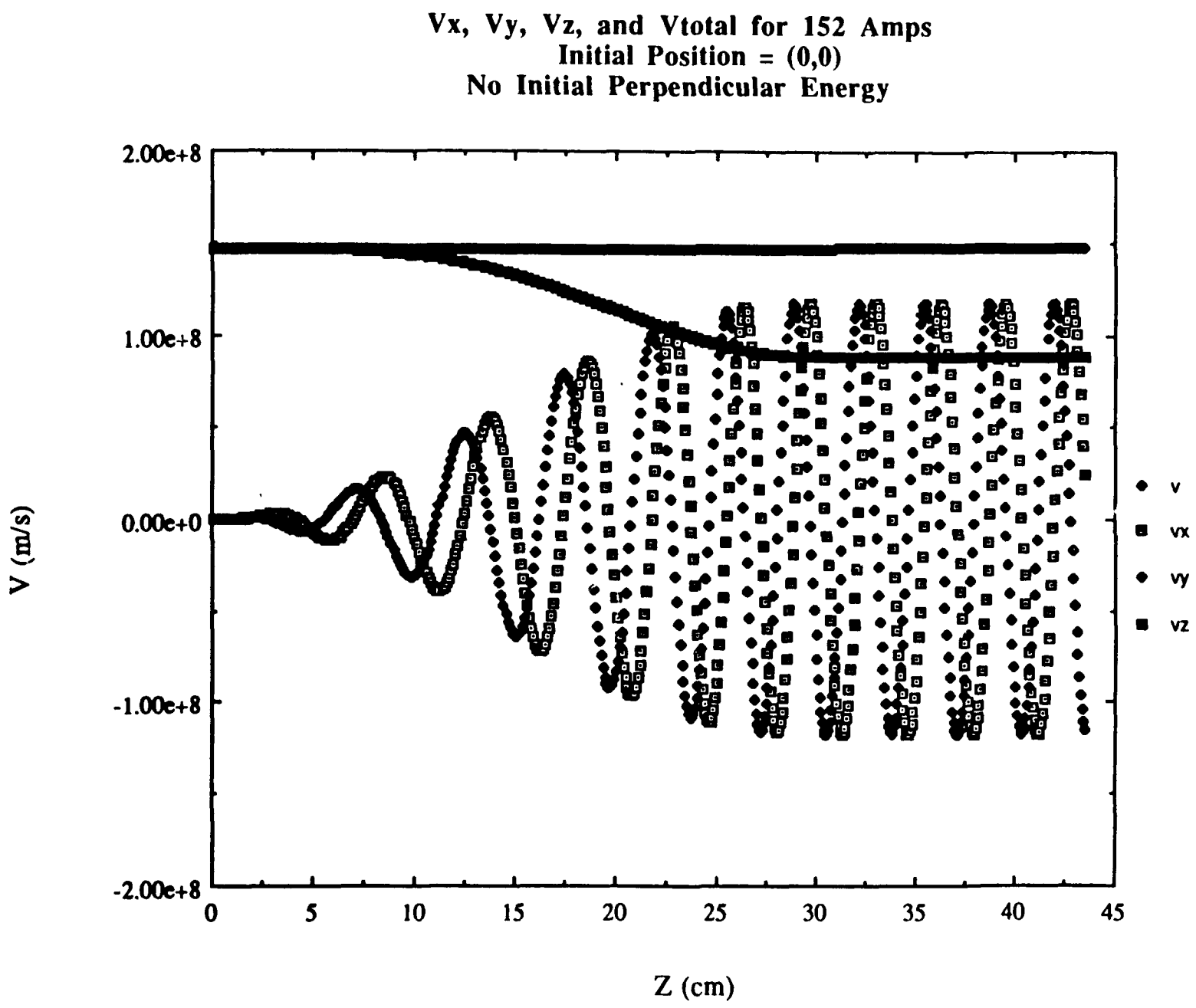
Vx, Vy, Vz, and Vtotal for 152 Amps
Initial Position = (0,0)
No Initial Perpendicular Energy
2.00e+8
1.00e+8
0.00e+0
-1.00e+8
-2.00e+8
V (m/s)
0
5
10
15
20
25
30
35
40
45
Z (cm)
v
vx
vy
vz

Figure 5.2

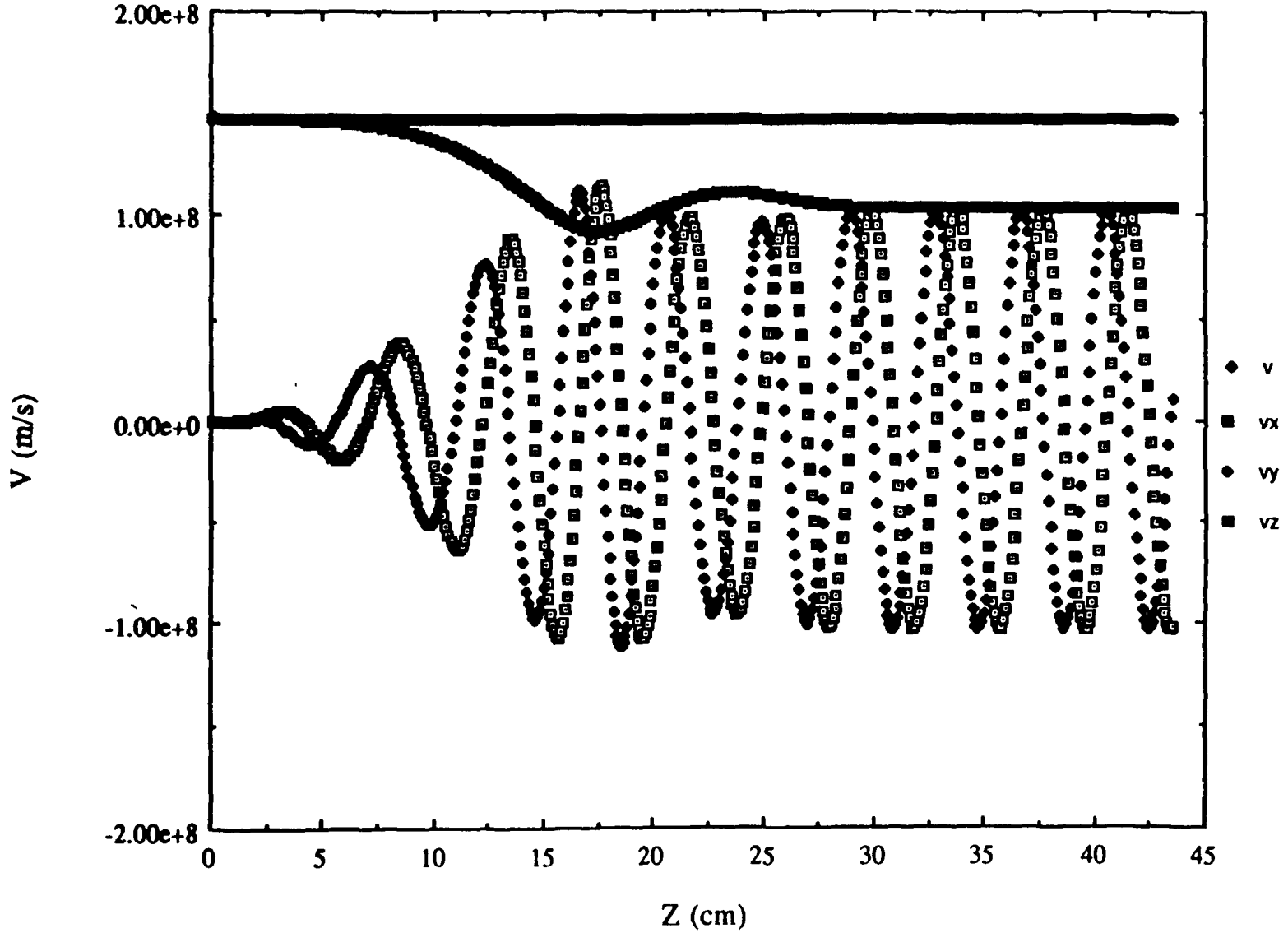
Vx, Vy, Vz, and Vtotal for 250 Amps
Initial Position = (0,0)
No Initial Perpendicular Energy
2.00e+8
1.00e+8
0.00e+0
-1.00e+8
-2.00e+8
V (m/s)
0
5
10
15
20
25
30
35
40
45
Z (cm)
v
vx
vy
vz

Figure 5.3

X vs. Y for 152 Amps
Initial Position = (0.7,0.1)
No Initial Perpendicular Energy

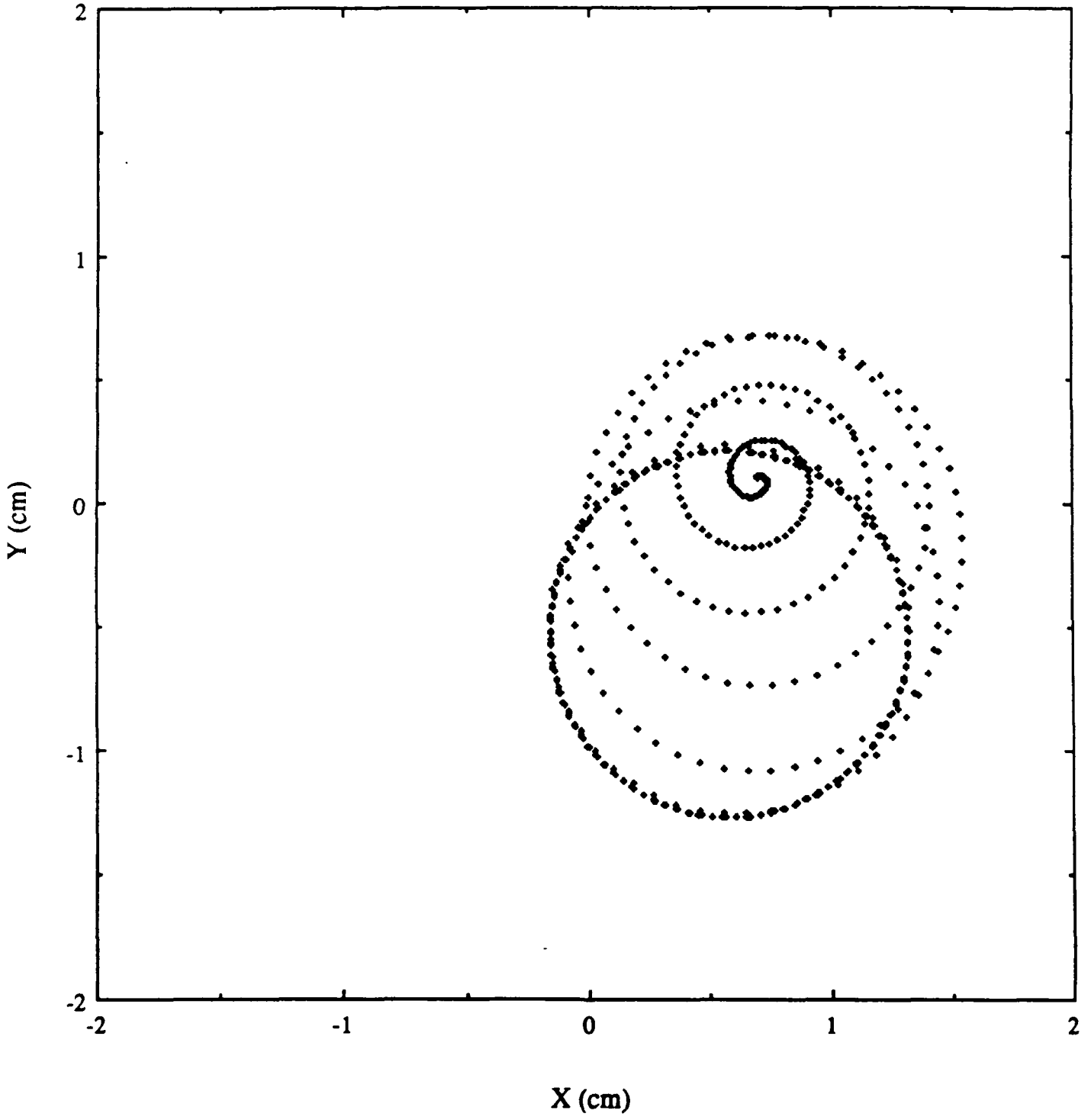

Figure 5.4

Vx, Vy, Vz, and Vtotal for 152 Amps
Initial Position = (0.1,0.1)
No Initial Perpendicular Energy

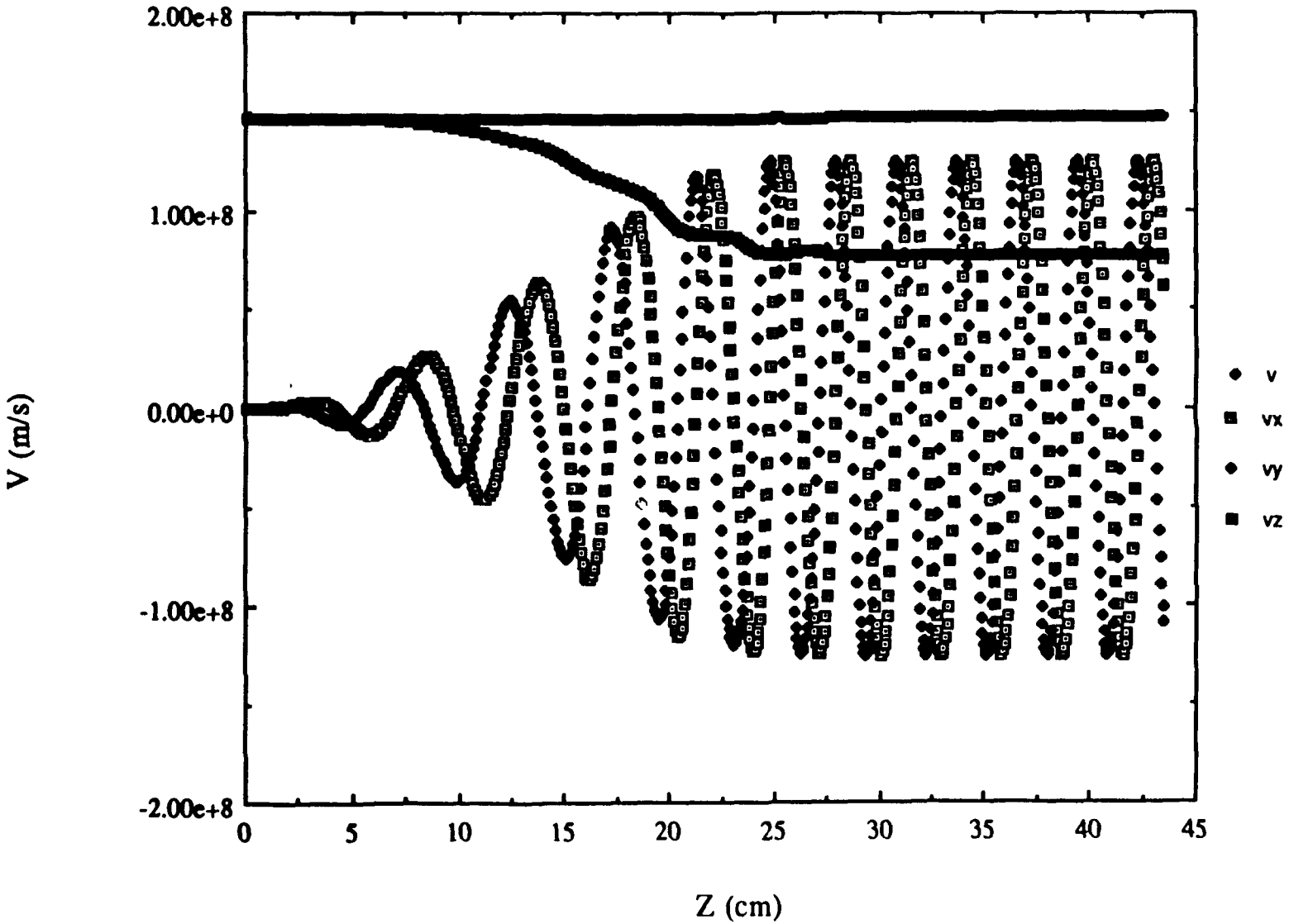

Figure 5.5

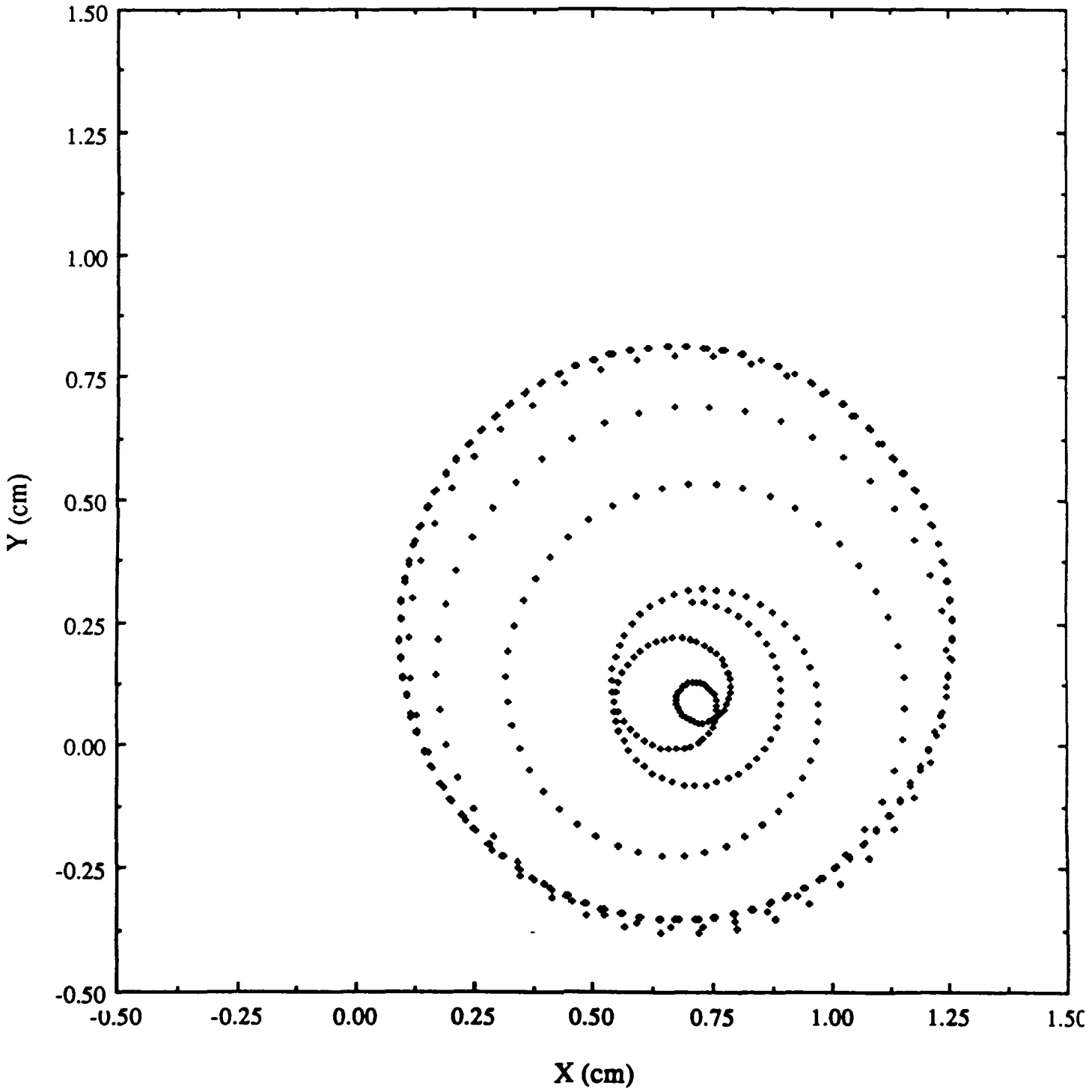
X vs. Y for 152 Amps
Initial Position = (0.7,0.1)
5 % Initial Perpendicular Energy
1.50
1.25
1.00
0.75
0.50
0.25
0.00
-0.25
-0.50
Y (cm)
-0.50
-0.25
0.00
0.25
0.50
0.75
1.00
1.25
1.5C
X (cm)

Figure 5.6

Vx, Vy, Vz, and Vtotal for 152 Amps
Initial Position = (0.7,0.1)
5 % Initial Perpendicular Energy

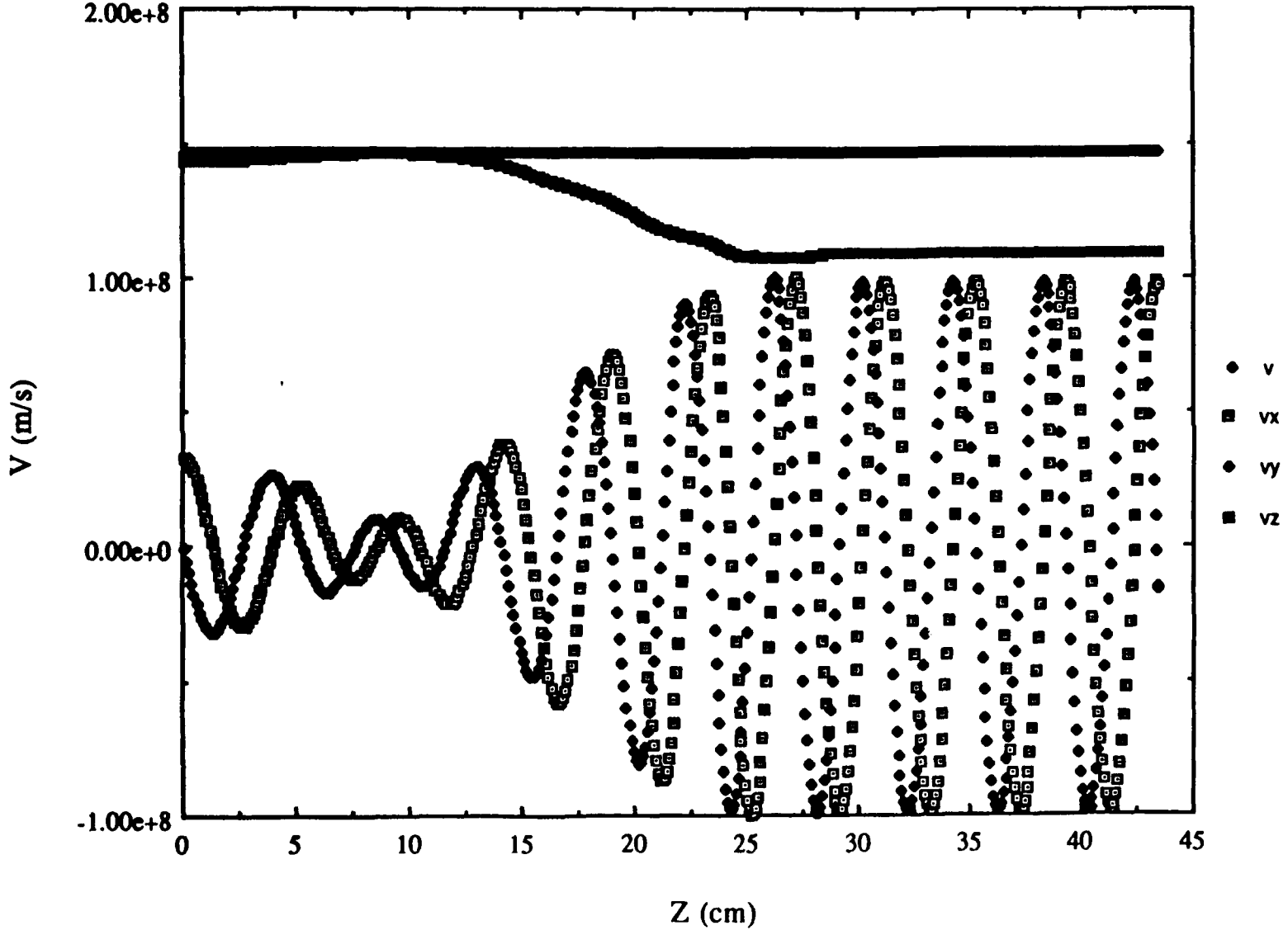

Figure 5.7

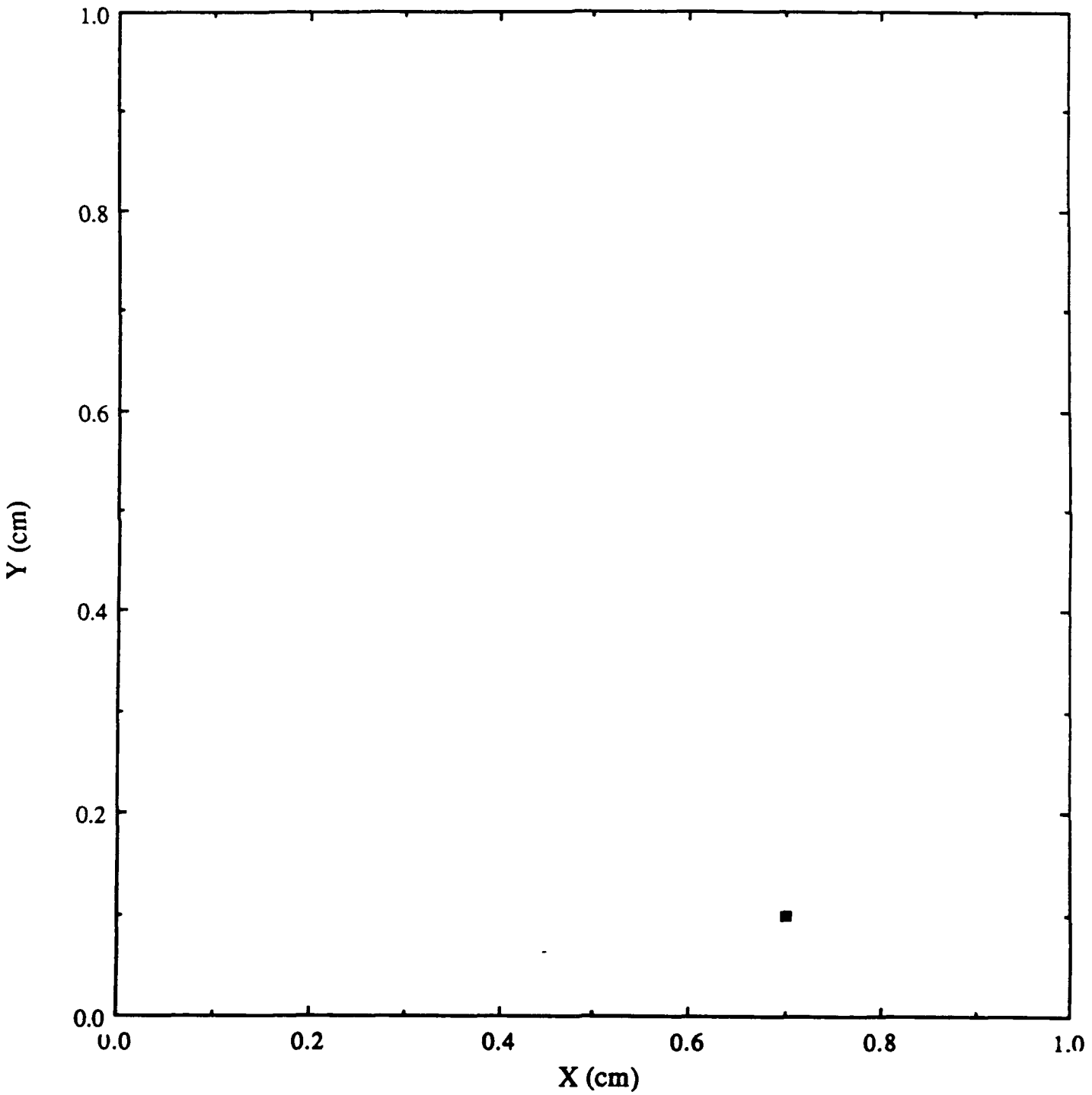
X vs. Y for 0 Amps
Initial Position = (0.7,0.1)
No Initial Perpendicular Energy
1.0
0.8
0.6
0.4
0.2
0.0
Y (cm)
0.0
0.2
0.4
0.6
0.8
1.0
X (cm)

Figure 5.8

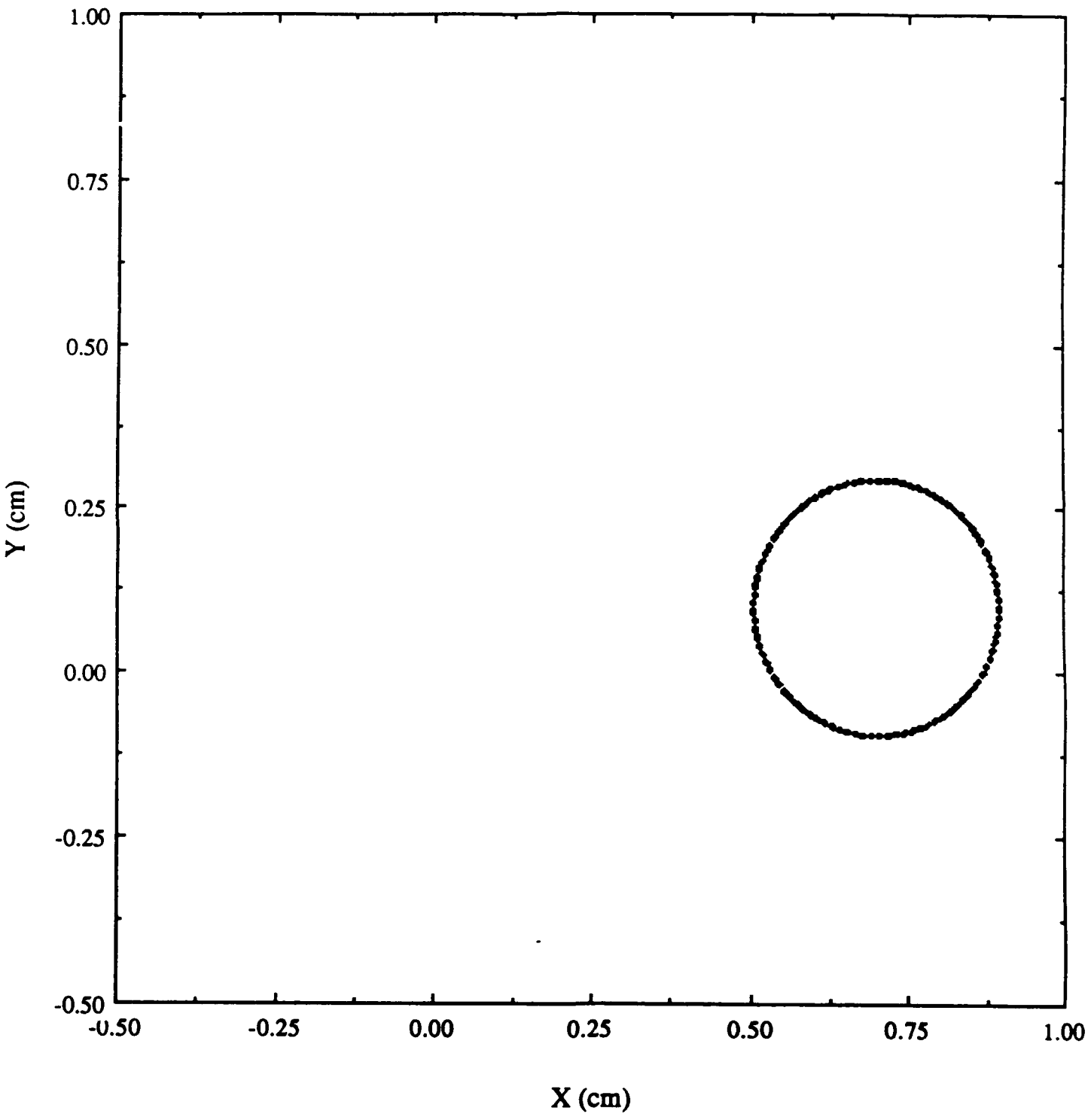
X vs. Y for 0 Amps
Initial Position = (0.7,0.1)
5 % Initial Perpendicular Energy
1.00
0.75
0.50
0.25
0.00
-0.25
-0.50
Y (cm)
-0.50
-0.25
0.00
0.25
0.50
0.75
1.00
X (cm)

Figure 5.9

VI. Conclusions

The computer served as a valuable tool in the design of the wiggler. Due to the relative ease with which new plots are generated, it is possible to design and construct a number of different wigglers to suit different operating conditions. Also, with the aid of the electron trajectory program, it is possible to track the electrons through any wiggler design before actually building the wiggler itself, thereby ensuring a perfect match to the operating beam system.

Appendix A
Comments on the wiggler design program

The computer program is based on the work of Ajit Singh in his thesis, Generation and Wave Propagation Characteristics of Spiraling Electron Beams. The main modifications involved the addition of the MTS plotting routines to produce the plot used in constructing the wiggler. Following is a summary of the mechanics of the program. There are also detailed comments contained in the program listing itself, which is included at the end of this appendix.

The program calculates the physical positioning of the wires, as well as the current needed to drive the wiggler based upon the following input parameters : (The values used for our wiggler are shown in parenthesis).

ALPH =	(0.8316)	Windup Ratio
ELLCM =	(30)	Length of the Wiggler in cm.
BG =	(1100)	Axial Magnetic field in Gauss
CHI =	(0)	Initial phase angle of the electron
EZERO =	(75,000)	Electron Injection Energy in ev
RHCM =	(1.90)	Radius of the wiggler in cm.

The program calculates the position of the two pairs of wires. This data is then sent to the MTS calcomp plotter, which generates an exact scale drawing of the wire position on the wiggler.